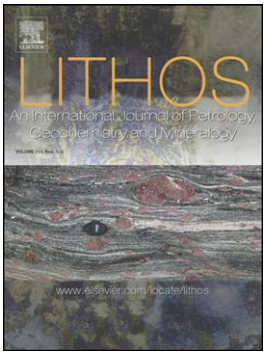

Petrogenetic significance of ocellar camptonite dykes in the Ditrău Alkaline Massif, Romania

Anikó Batki, Elemér Pál-Molnár, Gábor Dobosi, Alasdair Skelton

PII: S0024-4937(14)00156-X
DOI: doi: 10.1016/j.lithos.2014.04.022
Reference: LITHOS 3273

To appear in: *LITHOS*

Received date: 20 January 2014
Revised date: 28 April 2014
Accepted date: 29 April 2014

Please cite this article as: Batki, Anikó, Pál-Molnár, Elemér, Dobosi, Gábor, Skelton, Alasdair, Petrogenetic significance of ocellar camptonite dykes in the Ditrău Alkaline Massif, Romania, *LITHOS* (2014), doi: 10.1016/j.lithos.2014.04.022

Petrogenetic significance of ocellar camptonite dykes in the Ditrău Alkaline Massif, Romania

Anikó Batki[a*], Elemér Pál-Molnár[a,b], Gábor Dobosi[a,c], Alasdair Skelton[d]

[a]MTA-ELTE Volcanology Research Group, H-1117 Budapest, 1/C Pázmány Péter street, Hungary, e-mail: batki@geo.u-szeged.hu

[b]Department of Mineralogy, Geochemistry and Petrology, University of Szeged, H-6722 Szeged, 2 Egyetem street, Hungary

[c]Institute for Geological and Geochemical Research, Research Centre for Astronomy and Earth Sciences, Hungarian Academy of Sciences, H-1112 Budapest, 45 Budaörsi street, Hungary

[d]Department of Geological Sciences, Stockholm University, SE-10691 Stockholm, Sweden

Abstract

Camptonite dykes intrude the rift-related Mesozoic igneous body of the Ditrău Alkaline Massif, Eastern Carpathians, Romania. We present and discuss mineral chemical data, major and trace elements, and the Nd isotopic compositions of the dykes in order to define their nature and origin. The dykes are classified as the clinopyroxene-bearing (camptonite–I) and clinopyroxene-free (camptonite–II) varieties. Camptonite–I consists of aluminian–ferroan diopside phenocrysts accompanied by kaersutite, subordinate Ti-rich annite, albite to oligoclase and abundant calcite–albite ocelli. Camptonite–II comprises K-rich hastingsite to magnesiohastingsite, Ti-rich annite, albite to andesine, abundant accessory titanite and apatite, and silicate ocelli filled mainly with plagioclase (An_{4-34}).

Age-corrected $^{143}Nd/^{144}Nd$ ratios vary from 0.51258 to 0.51269. The high ε_{Nd} values of +4.0 to +6.1 which are consistent with intra-plate composition, together with light rare earth element (LREE), large ion lithophile element (LILE) and high field strength element (HFSE) enrichment in the camptonites is ascribed to the formation of small melt batches of a metasomatised sub-lithospheric mantle source. The presence of an asthenospheric 'high μ' ocean island basalt (HIMU–OIB)-type mantle component in the source region has also been revealed. A 1–4% degree of partial melting of an enriched garnet lherzolite mantle source containing pargasitic amphibole followed by fractionation is inferred to have been involved in the generation of the camptonites. They are deduced to be parental melts to the Ditrău Alkaline Massif.

Keywords: Camptonite; Ocelli; Metasomatised sub-lithosphere; HIMU–OIB mantle component; Intra-plate magmatism; Ditrău Alkaline Massif

1. Introduction

Camptonitic alkaline lamprophyres are usually associated with alkaline syenite-gabbro plutons (e.g. Monteregian Hills, Canada). In many occurrences, such as Borralan (Scotland), Lovozero and Khibina (Kola Peninsula, Russia), and Sokli (Finland) (Rock, 1991 and references therein) they are the most primitive or the only primitive rocks, or represent the only primitive melts to penetrate throughout some provinces (e.g. Monteregian; Iberian, Gorringe Bank). As such, lamprophyres have now been equated with parental melts for a wide range of igneous suites generated repeatedly in time and space (Mitchell, 1994; Rock, 1991). Alkaline lamprophyres are widely recognised at divergent margins (rift valleys, triple junctions) and in intra-plate (oceanic islands, hot-spots) tectonic settings, and they are genetically associated with alkali basaltic magmatism (e.g. Kerr et al., 2010; Orejana et al.,

2008; Tappe et al., 2006). Alkaline lamprophyres are more typical of uncontaminated, primary mantle-derived rocks generated at considerable depths (100–150 km) (e.g. Bédard, 1994; Bernard-Griffiths et al., 1991). They frequently contain carbonate ocelli which may suggest the presence of CO_2 in their upper-mantle source. Thus their study can put additional constrains on the role of CO_2-H_2O-rich fluids during mantle metasomatism (Bouabdli et al., 1988; Hidas et al., 2010).

Numerous camptonite dykes occur in the northern part of the Ditrău Alkaline Massif, Eastern Carpathians (Romania), intruding hornblendite, diorite, nepheline syenite, syenite, and granite. Petrogenetically, neither of the lamprophyres has been studied, although they are widely reported in previous papers on the geology of the massif (Kräutner and Bindea, 1998; Streckeisen, 1954, 1960; Streckeisen and Hunziker, 1974); only a few studies have dealt with the petrography and mineralogy of the lamprophyres and a few have given some whole-rock chemical data (Anastasiu and Constantinescu, 1982; Fellner, 1867; Mauritz, 1912; Streckeisen, 1954; Vendl, 1926) but no interpretation of their origin.

This paper provides new data on mineralogy, mineral chemistry and major, trace, and rare-earth element whole-rock chemistry, as well as on the Sr-Nd isotopic compositions of the Ditrău camptonites, a set of mafic alkaline volatile-rich intrusions that cross-cut the Ditrău Alkaline Massif. The camptonites have the potential to provide important information on the mantle geochemistry beneath the region of their emplacement and on the origin of parental melts of the massif.

2. Geological setting

The Ditrău Alkaline Massif in the Eastern Carpathians (Romania) is a Mesozoic alkaline igneous complex (19 km long and 14 km wide, ca. 200 km^2 in size on the surface, Pál-Molnár, 2000). In the structural system of the Alpine–Carpathian–Dinaric region it belongs to

the Dacia Mega-Unit (Fig. 1A). The massif intrudes Variscan metamorphic rocks which can be identified in the Alpine Bucovinian Nappe, Eastern Carpathians (Săndulescu, 1984). These Variscan nappes are built up by the Bretila lithogroup (Rarău Nappe), Rebra lithogroup (Rodna Nappe) and Tulghes lithogroup (Putna Nappe) (Balintoni, 1994) (Fig. 1B). The Bucovinian Nappe represents the upper unit of the Central Eastern Carpathian nappes, which formed during the Middle Cretaceous (Săndulescu, 1984). It is partly covered by Neogene-Quaternary andesitic pyroclasts and lava flows of the Călimani–Gurghiu–Harghita volcanic chain and by Pliocene–Pleistocene sediments and lignite-bearing lacustrine deposits of the Gheorgeni and Jolotca Basins (Codarcea et al., 1957; Fig. 1B).

The massif comprises a series of ultramafic to mafic rocks in the north- and central-west (hornblendite, gabbro and diorite), felsic silica-saturated and silica-oversaturated syenites and granites (from the north to the south-east), as well as silica-undersaturated alkaline rocks dominating the central and the eastern part (Fig. 1B). Numerous dykes, including lamprophyres, tinguaites, alkali feldspar syenites and nepheline syenites, cut the whole complex.

In the last 180 years, the Ditrău Alkaline Massif has been the subject of many investigations (Anastasiu and Constantinescu, 1982; Codarcea et al., 1957; Dallmeyer et al., 1997; Fall et al., 2007; Jakab, 1988; Kräutner and Bindea, 1998; Mauritz, 1912; Morogan et al., 2000; Pál-Molnár, 2000; and references therein). However, because of its structural complexity and wide petrographic variability the petrogenesis is still not completely understood. Proposed petrogenetic models range from metasomatic to magmatic origin and from emplacement in a single magmatic event to multiple successive magmatic pulses. Detailed descriptions of these models are given by Morogan et al. (2000).

Ultramafic rocks in the north- and central-west represent the earliest intrusive phases. Pál-Molnár and Árva-Sós (1995) using K/Ar ages on hornblende, biotite, nepheline and feldspar

separates, gave dates of 216–237 Ma for hornblendites, 234 Ma for gabbros, 216–232 Ma for nepheline syenites, 196–217 Ma for granites and 102–113 Ma for syenites.

Providing two additional $^{40}Ar/^{39}Ar$ hornblende ages of 231 Ma and 227 Ma for gabbro and diorite, respectively, Dallmeyer et al. (1997) confirmed the middle- to late-Triassic age of these early components. Pană et al. (2000) reported the U-Pb zircon emplacement age from the syenite of 229.6±1.7 Ma and suggested that the syenite and associated granite were formed by crustal melting during the emplacement of the mantle-derived gabbroic magma around 230 Ma. Morogan et al. (2000) suggested a basanitic OIB-like character for the parent magma, generated by small degrees of melting of asthenospheric garnet lherzolite and that the multistage intrusions were caused by a mantle plume; they attribute an important role to assimilation and fractionation, the mixing of salic and basaltic melts and the relatively hydrous nature of the Ditrău magmas.

3. Field relations and samples

Lamprophyre intrusions are quite common in the whole area of the Ditrău Alkaline Massif. They cross-cut the main intrusions of the massif, hornblendite, nepheline syenite and syenite, and granite, and are themselves cut by alkali feldspar syenite dykes and veins (Fig. 2). The lamprophyre dykes have sharp contact with the host rocks and some of them show very thin chilled margins. Locally all the rocks are more or less altered. Some lamprophyres are disintegrated mostly at the margins of the dykes (Fig. 2A). The dykes are up to several metres long, range in width from 20 cm to 2 m, and strike in a general east or northeast direction. Some of the faults which cut the massif also crosscut the lamprophyre dykes. They are melanocratic rocks and are greenish-grey to dark grey in colour. Large biotite flakes up to 5 mm in diameter and locally abundant felsic globular textures, ocelli reaching 1 cm in diameter, are visible to the naked eye (Fig. 2B).

Since the occurrence of lamprophyre dykes and their contact with other rock types in the natural outcrops can be found and studied best in the northern part of the Ditrău Massif, the Jolotca Creek and its northern effluents (Tarnița, Teasc, Filep, Gudu, Turcului and Creangă Mare Creeks) have been chosen as the studied area. Forty-five samples were collected from ten dykes exposed in surface outcrops. These localities are shown in Figure 1C.

4. Analytical methods

Eighteen lamprophyres were selected for whole-rock chemical analyses, seven samples were analysed for their mineral composition and four were analysed for Sr and Nd isotope compositions. The samples were selected to cover the range of mineralogical varieties of the lamprophyres in a representative way.

Minerals were analysed with a Cameca SX50 electron microprobe in wavelength-dispersion mode at the Department of Geosciences, Uppsala University, Sweden, using a beam current of 15 nA and an acceleration voltage of 20 kV. Standards used were albite (Na), periclase (Mg), corundum (Al), wollastonite (Ca, Si), orthoclase (K), pyrophanite (Mn, Ti) and magnetite (Fe). Counting times were 10–30 s for peaks and 10 s for background. Data correction was carried out using online PAP Cameca Software. Additional electron microprobe work on all the main rock-forming phases was performed at the Institute for Geological and Geochemical Research, Research Centre for Astronomy and Earth Sciences, Hungarian Academy of Sciences, Budapest, Hungary using a JEOL Superprobe 733 operated at an acceleration voltage of 20 kV and a beam current of 15 nA. At the same place, cathodoluminescence studies were carried out on carbonate ocelli using Reliotron cold-cathode equipment mounted on a Nikon E600 microscope operated at 5–7 kV accelerating voltage and 0.5–1.0 mA current.

Whole-rock major element compositions were analysed with an ICP mass spectrometer (Finnigan MAT Element) and trace elements were determined by ICP atomic emission spectrometry using a Varian Vista AX spectrometer at the Department of Geological Sciences, University of Stockholm, Sweden.

Sr and Nd isotope compositions were obtained at the Laboratory of Isotope Geology, Swedish Museum of Natural History, Stockholm, Sweden. Sr, Sm and Nd were loaded on Re double filaments and analysed on a Finnigan MAT261 thermal ionisation mass spectrometer (TIMS), equipped with a multi-collector system encompassing five Faraday detectors. $^{87}Sr/^{86}Sr$ measurements were corrected for possible ^{87}Rb interference, and for mass fractionation by normalisation to $^{86}Sr/^{88}Sr=0.1194$. $^{143}Nd/^{144}Nd$ measurements were corrected for possible ^{144}Sm interference, and for mass fractionation by normalisation to $^{146}Nd/^{144}Nd=0.7219$. One run of the NBS SRM 987 Sr standard during the measurements yielded $^{87}Sr/^{86}Sr=0.710236\pm24$ ($2\sigma_m$), whereas one run of LaJolla Nd standard gave a $^{143}Nd/^{144}Nd$ ratio of 0.511859 ± 11 ($2\sigma_m$). Initial $^{87}Sr/^{86}Sr$ and $^{143}Nd/^{144}Nd$ ratios were calculated for an age of 200 Ma, on the basis of K/Ar ages on hornblende, biotite and nepheline from hornblendite, gabbro, nepheline syenite and granite of the Ditrău Alkaline Massif (Pál-Molnár and Árva-Sós, 1995).

5. Results

5.1. Petrography

The lamprophyres are fine grained with a typical hypocrystalline porphyritic and panidiomorphic texture, but mineralogically they differ from each other. There are clinopyroxene-bearing and clinopyroxene-free varieties. Major components of both types are amphibole, biotite and plagioclase. Olivine is totally decomposed to green or colourless secondary amphibole in radiating nests. According to their mineral assemblage, the studied

lamprophyres are camptonites (Le Maitre, 2002; Rock, 1991). A characteristic feature of the camptonites is the presence of abundant spherical or ellipsoidal leucocratic globules, ocelli, 0.1–11 mm in size. Compositionally, camptonite–I (clinopyroxene-bearing) and camptonite–II (clinopyroxene-free) contain different types of ocelli.

The studied camptonites do not contain any kind of xenoliths: only occasional plagioclase xenocrysts can be found in a few samples. Veins filled with carbonate, epidote, sulphide and oxide minerals are present in the camptonite dykes.

5.1.1. Camptonite–I

Camptonite–I dykes occur in Jolotca, Tarnița and Turcului Creeks (Fig. 1C). The dykes have clinopyroxene phenocrysts range from subhedral to anhedral, set in a groundmass of brown amphibole, subordinate biotite, anhedral plagioclase, accessory acicular apatite, opaque minerals and titanite. The 0.6- to 2.4-mm-diameter clinopyroxene phenocrysts (ca. 1–10%) vary in abundance, and have been extensively replaced by an assemblage of tremolite to actinolite, and biotite (Fig. 3A). Olivine in fresh state is absent. In all cases they are totally replaced by tremolite and actinolite ± chlorite ± calcite ± epidote ± opaque phases, and only fine-grained light-green-coloured or colourless pilitic pseudomorphs show their previous presence (up to 15%). These late-stage or subsolidus alterations of primary phenocrysts are developed to an extreme degree, due to their high volatile content (Rock, 1991). All brown hornblendes (0.3–1.8 mm in size) are zoned having a thin, greenish rim. They dominate over biotite. Biotite is represented by small bladed, subhedral crystals which are usually chloritised. Interstitial plagioclase fills up residual places between mafic components. It is subhedral to anhedral and variably sericitised. There are two types of ocelli, even within the same sample. The first type contains sparry carbonate minerals together with biotite or titanite, and/or oxide and sulphide minerals in the interior with albite occurring in the rim.

Groundmass biotite is often aligned tangentially to the rim of ocelli (Fig. 3B). Neither feldspathoid nor zeolite (e.g. analcime) minerals appear as would be expected in a camptonite. Some of the euhedral calcite crystals in the interior of these ocelli can reach a size of 2.7 mm (Fig. 3B, F). The second type contains abundant plagioclase with a minor amount of calcite, amphibole and biotite. Here, plagioclases are strongly zoned, and epidote grains occur in their core. At zone boundaries of the plagioclase core epidote forming always stops where probably the necessary amount of calcium for epidote runs out from the Ca-rich plagioclase core. Well crystallised grains or aggregates of carbonate–chlorite–epidote in lamprophyres (Fig. 3C) form, particularly in globular structures (e.g. Rock, 1991).

5.1.2. Camptonite–II

Camptonite–II dykes occur in Teasc, Filep, Gudu, Turcului and Creangă Mare Creeks (Fig. 1C). They lack clinopyroxene and pseudomorphs of olivine, but do have subordinate hornblende phenocrysts settled in a groundmass composed of abundant green amphibole, biotite, interstitial plagioclase, accessory euhedral apatite, titanite and opaque minerals. The few amphibole phenocrysts are up to 2.4 mm in size. Both phenocryst and groundmass amphiboles form euhedral to subhedral prisms and needles, often displaying preferred orientation due to magma flow and contain magnetite needles indicating magmatic resorption of amphiboles. In some cases, the groundmass shows banded internal structures indicating flow differentiation, or multiple intrusions (e.g. Upton, 1965). The intergrowth of amphibole and biotite indicates their simultaneous crystallisation (Fig. 3G). The matrix is variably altered (i.e. chloritised and sericitised). Ocelli are made up of silicates (plagioclase with subordinate amphibole, biotite and zoned titanite) and euhedral accessory apatite. Amphibole occurs tangentially in the rim of the ocelli (Fig. 3D). Titanite, which is ubiquitous in all other

Ditrău rocks, is more abundant in camptonite–II than in camptonite–I. Titanite and apatite grains in the ocelli are distinctly larger than those in the groundmass.

5.2 Mineral chemistry

5.2.1. Clinopyroxene

Representative analyses are shown in Table I of the electronic supplement. Due to the complete alteration of olivine in camptonite–I, their composition could not be determined therefore clinopyroxene is the only measurable phenocryst phase in these dykes. It is classified in terms of quadrilateral components (Morimoto, 1988) and is principally of aluminian–ferroan diopside with a narrow compositional range of $Di_{76-93}Hd_{1-19}Aeg_{2-8}$ (Table 1). Well defined zoning can not be identified within individual clinopyroxene grains due to the different degree of alteration. Compositions of cores and rims overlap (Fig. 4). All the diopsides exhibit high Al and Ti content (up to 7.93 wt. % Al_2O_3 and up to 3.30 wt. % TiO_2), similar to the clinopyroxenes of the Catalonian (Ubide et al., 2012), Spanish Central System (Orejana et al., 2008) and Río Grande (Hauser et al., 2010) lamprophyres and those of the Carpathian–Pannonian Region lamprophyres (Harangi et al., 2003; Szabó et al., 1993). The highest Di-content belongs to chromian diopsides (up to 0.81 wt. % Cr_2O_3). Most clinopyroxene compositions show a clear differentiation trend, with slight to strong positive correlations between Al and Ti, Mg and Si, and Cr and mg#, and negative correlations between Mg and Al, Ti, and $Ti+Al^{IV}$ and Si (Fig. 4).

5.2.2. Amphibole

Amphibole is mostly a groundmass phase in the studied camptonites occurring as microcryst. Besides, some phenocrysts appear in camptonite-II. Amphibole is kaersutite with a

magnesiohastingsite rim in camptonite–I and hastingsite in camptonite–II (Table II of the electronic supplement) according to Leake et al. (1997).

Kaersutite is characterised by high Ti and relatively low Al content (TiO_2=5.1–7.1 wt. %; Al_2O_3<13.6 wt. %), similar to the amphiboles of the Monteregian (Bédard, 1988), Tamazert (Bouabdli et al., 1988), Pyrenean (Azambré et al., 1992), Moravian-Silesian, Mecsek-Alföld (Harangi et al., 2003) and Catalonian (Ubide et al., 2012) lamprophyres. Compositional trends for kaersutites are consistent with early crystallisation from Si-undersaturated magma (Bédard, 1988; Giret et al., 1980). Kaersutite cores yield more primitive compositions while magnesiohastingsite rims show more evolved compositions, with decreasing Ti and Al^{IV} p.f.u. and increasing Si and Fe^{tot} p.f.u. for decreasing mg# from the core towards the rim (Fig. 5); thus, magnesiohastingsite rims seem to have crystallised from a slightly more evolved magma or under different conditions.

Both phenocryst and groundmass hastingsite in camptonite–II have high Fe and K p.f.u. contents (FeO^{tot}=18–20 wt. % and K_2O=1.0–2.1 wt. %). They also have lower Ti and higher K p.f.u. concentrations than kaersutite in camptonite–I (Fig. 5), indicating slightly higher pressure conditions (Adam and Green, 1994). Most hastingsite contains secondary magnetite needles indicating magmatic resorption of the amphibole during magma ascent.

5.2.3. Biotite

In camptonite–I, three generations of biotite are present: groundmass minerals, ocellus biotites (primary phases) and the breakdown products of clinopyroxene phenocrysts (secondary phases). In contrast, in camptonite–II there are only groundmass and ocellus biotite. Groundmass and ocellus biotite is annite (mg#=0.47–0.62) in all of the camptonites, while the breakdown products of clinopyroxenes are phlogopites (mg#=0.65–0.73). As for clinopyroxenes and amphiboles, the high Ti content (TiO_2=1.7–3.0 wt. %) is a characteristic

feature of biotites, similar to the biotites of the Tamazert alkaline lamprophyres (Bouabdli et al., 1988) and those of the Carpathian–Pannonian Region lamprophyres (Harangi et al., 2003; Szabó et al., 1993). Biotites in both types of camptonite have moderate to high Al content (Al_2O_3=14.0–16.3 wt. %), while Ti and Fe concentrations are higher (Table III of the electronic supplement) in camptonite–II.

5.2.4. Carbonate

Carbonate is calcite and appears in camptonite–I, mostly as ocellus, groundmass and vein mineral, but does also occur in pilitic pseudomorphs after olivine. The large ocellus calcite (up to 2.7 mm in size) coexists with titanite or albite, biotite ± oxide and/or sulphide phases (Fig. 3B, F). Cathodoluminescence images of calcites show a homogeneous texture and a lighter orange colour at the rims than in the cores (Fig. 3E, F) which reflect their variable Mn and/or REE content. It is generally accepted that Mn^{2+} and mostly trivalent REEs are the most important activators of extrinsic CL in carbonate minerals, while Fe^{2+} is a quencher of CL (e.g. Machel, 2000). Cathodoluminescence images also reveal that carbonate veins intersect both carbonate ocelli, and the pilitic pseudomorphs after olivine phenocrysts (Fig. 3E).
In camptonite–II calcite is present only in ocelli as an accessory phase together with late-stage hydrothermal barite (Fig. 3H).

5.2.5. Feldspar

The feldspars are mostly plagioclases with anorthite content of An_5 to An_{28} in camptonite–I and An_4 to An_{34} in camptonite–II, corresponding to albite, oligoclase and andesine (Table III of the electronic supplement). They are present as ocelli minerals and interstitial grains in the groundmass. In silica-rich ocelli (camptonite–II) plagioclases are zoned with andesine cores and oligoclase to albite rims and have the same composition as the groundmass ones. In

contrast, in carbonate-rich ocelli (camptonite–I) albite is present and groundmass feldspars are albite to oligoclase in composition.

5.3. Geochemistry

5.3.1. Major and trace element geochemistry

Geochemical descriptions for the major element composition of the Ditrău camptonites (four samples) were previously published by Mauritz (1912) and Vendl (1926). Morogan et al. (2000) also gave major, trace and REE data of two dykes, one basanite and one alkali basalt (Table 1). In this study, new analyses for major, trace and REEs include eighteen camptonites (Table 1).

In general, there is no significant difference between the chemical composition of camptonite–I and camptonite–II (Fig. 6, Table 1). The Ditrău camptonites are high in alkalis (Na_2O+K_2O=5.3–8.1), TiO_2 and P_2O_5 but low in SiO_2 (Table 1), a feature common to mafic alkaline rocks. The high Ti/V (>50), low Y/Nb (<1) and chondrite-normalised $(La/Yb)_n$ (>11) ratios are also consistent with the alkaline character (according to Pearce and Cann, 1973; Rock, 1991).

In the TAS diagram (Le Maitre et al., 2002), the Ditrău camptonites plot as basanites and trachy-basalts. Except for one sample of VRG7305, they are moderately to strongly Si-undersaturated with 3–14% nepheline in the norms, do not contain normative hypersthene or quartz, and also lack normative leucite. Sample VRG7305 from the camptonite–II is Si-saturated with normative hypersthene (hy=22%). Camptonite–I is slightly more Si-undersaturated (ne=8–14%) than camptonite–II (ne=0–10%). Sodium dominates over potassium, with Na_2O/K_2O varying from 1 to 3. Mg values ($(Mg/Mg+Fe^{2+})$ with Fe^{2+} according to Irvine and Baragar, 1971) vary from 0.44 to 0.70, indicating moderate mineral fractionation, and positive correlation with abundances of compatible elements (Cr, Ni, Co

and Sc, Fig. 7), consistent with extraction of olivine and clinopyroxene in the early stage of evolution. CaO and FeO^t decrease with decreasing mg values (Fig. 6) suggesting the fractionation of clinopyroxene and calcic amphibole. TiO_2 and V increase up to mg# of about 0.5 and then decrease in both camptonite with mg#<0.5 (Figs. 6, 7), suggesting the fractionation of titanite and kaersutite. Al_2O_3 and Na_2O increase with increasing SiO_2 as a result of feldspar fractionation which is mainly albite to oligoclase (Fig. 6).

The high Nb concentrations in the Ditrău camptonites are notable, with most of the analysed samples having contents ≥100 ppm (Table 1). The Zr and Hf contents are also high and fall within the range of alkaline lamprophyres (Rock, 1991). Nb, Hf and Y increase with differentiation (Fig. 7). The Zr/Hf and Zr/Nb ratios of camptonite–II correlate well with the Zr concentrations (R^2=0.89 and R^2=0.75, respectively). Nb/La and Th/La ratios are constant with the averages of 1.5±0.2 and 0.135±0.03, respectively. These values agree well with the data for alkaline lamprophyres (Rock, 1991). Most of the Zr/Hf ratios (21.0–32.2) are significantly lower than the chondritic ratio of 34.2 (Weyer et al., 2002). There are some exceptions with Zr/Hf ratios of 35.7–45.7 (VRG7286, VRG7287, VRG7296 and VRG7297).

The studied camptonites are also rich in alkali (Rb=72–499 ppm) and alkali earth elements, with Ba and Sr reaching concentrations of 3020 ppm and 1411 ppm, respectively. In particular, there is a strong positive anomaly for Rb relative to the primitive mantle especially in samples VRG7286, VRG7287 and VRG7289 of camptonite–II (Fig. 8A, B). Enrichments in LIL elements may point to the effect of alteration (observed late-stage or subsolidus alterations of primary phases in most samples). However, similarly high concentrations and extensive variations of LIL elements were also described from several lamprophyres (e.g. Azambré et al., 1992; Dostal and Owen, 1998; Rock, 1991; Szabó et al., 1993). K_2O, Rb, Ba and Sr show wide scatter with mg#, without obvious evolution with the differentiation, which can be explained by their mobility (Fig. 7). Compared to alkaline lamprophyres worldwide

(Rock, 1991), the Ditrău camptonites have significantly lower K/Rb and Ba/Rb ratios however they have similar values of Ba/La ratios.

Primitive mantle-normalised REE patterns are steeply sloping, typical of alkaline rocks, lack Eu anomaly and display a strong enrichment of LREE and significant fractionation of HREE with an La/Yb ratio ranging from 15 to 38 (Fig. 8D, E). These values are similar to those of the average alkaline lamprophyres (La/Yb=37; Rock, 1991). The absence of positive Eu anomaly supports the lack of crustal contamination (e.g. Srivastava and Chalapathi Rao, 2007). The REE content increases with the decrease in mg values but the increase is more distinct for La, Ce, Sm and Eu than for Yb (and Y), which results in a decrease in the Yb/Eu and Y/Ce ratios with differentiation (Fig. 7). Calcic amphibole can take up considerable Y (Bédard, 1994), thus the decrease in the Yb/Eu and Y/Ce ratios suggests fractionation of the amphibole (Bouabdli et al., 1988).

5.3.2. Isotope geochemistry

Four Ditrău camptonites together with a hornblendite, a diorite, a monzonite and a syenite from the Ditrău Alkaline Massif for comparison were analysed for Sr and Nd isotope ratios (Table 2).

The $^{87}Sr/^{86}Sr_i$ compositions of the Ditrău camptonites vary from 0.70148 to 0.70211 (Table 2). Hydrothermal activity and mineralisation in the massif are already well known from previous studies (e.g. Fall et al., 2007; Kräutner and Bindea, 1998; Streckeisen and Hunziker, 1974). The unreasonably low initial Sr values, below mantle value, and high Rb content (and thus, higher Rb/Sr ratios) are probably due to hydrothermal alteration. Since the Rb-Sr system is easily disturbed because of the mobility of Rb, it does not remain a closed system, which is not uncommon with disturbed samples showing such unreasonably low initial Sr values (White, 2009). Disturbance can be caused by crustal contamination or hydrothermal activity.

The studied camptonites most likely have undergone some disturbance in the Rb/Sr ratio by later hydrothermal alteration, making their initial Sr values uncertain. A small increase in the Rb/Sr ratio (by Rb gain or Sr loss) could lead to such low initial Sr values. Since neither Sm nor Nd is particularly mobile, initial ratios are relatively insensitive to weathering, therefore we rely more on the Sm-Nd results. The $^{143}Nd/^{144}Nd_i$ ratios have a variable range of 0.51258–0.51269 (Table 2). The age–corrected ε_{Nd} values of +4.0 to +6.1 of the Ditrău camptonites are within the range of other alkaline lamprophyres (e.g. Bernard-Griffiths et al., 1991; Dostal and Owen, 1998; Harangi et al., 2003; Orejana et al., 2008) and fall near to the average for alkaline lamprophyres worldwide published by Rock (1991) (Fig. 9). The high and relatively homogeneous initial ε_{Nd} values are typical of enriched intra-plate compositions and are comparable to values observed in continental alkaline volcanic suites from extension and rift settings (e.g. Andronikov and Foley, 2001; Dostal and Owen, 1998; Orejana et al., 2008; Tappe et al., 2006).

6. Discussion

6.1. Mantle source and enrichment processes

The Ditrău lamprophyres compositionally resemble basanites and trachy-basalts, although they seem to present volatile-rich equivalents of these rocks (e.g. Rock, 1991). They contain kaersutite or hastingsite, Ti-rich annite, albite, oligoclase, andesine, apatite, titanite and magnetite in the groundmass with silicate–carbonate or silicate ocelli ± Al-Fe-diopside phenocrysts and pilitic pseudomorphs after olivine. They are significantly enriched in volatile elements (H_2O, CO_2), in LILE and in LREE.

According to Rock's definition (1991) alkaline lamprophyres, thus camptonites, are considered to represent primary mantle-derived magmas generated at considerable depths (e.g. Bédard, 1994; Bernard-Griffiths et al., 1991; Rock, 1991). Mantle-derived magmas are

characterized by low Lu/Yb ratios of 0.14–0.16 (Sun and McDonough, 1989), whereas continental crust possesses comparatively higher Lu/Yb ratios (0.16–0.18). The high LILE (e.g. Ba, Sr, Zr and Nb), LREE and low HREE, together with low Lu/Yb ratios of 0.12–0.16 and the absence of positive Eu anomaly point to the lack of crustal contamination in the studied camptonites.

The small variation in trace and REE characteristics implies that the Ditrău camptonites are formed by variable degrees of partial melting of the same mantle source. Since Y and the HREE are compatible in garnet, the depletion of these elements in camptonites is consistent with low degree fractional melting in a garnet-bearing source region (e.g. Downes et al., 2005; Koglin et al., 2009; White, 2009). The primitive mantle-normalised Sm/Yb ratios in the Ditrău camptonites vary between 2.1 and 4.9, confirming the presence of residual garnet during melting processes (e.g. McKenzie and O'Nions, 1991; Orejana et al., 2008). The high concentrations of incompatible elements indicate a metasomatised mantle source previously enriched in LILE and HFSE (e.g. Beard et al., 1996; Bouabdli et al, 1988; Hauser et al., 2010). In general, a relative depletion in Nb, Ta and/or Ti is typical of arc rocks; therefore, the absence of a significant Nb–Ta negative anomaly in the Ditrău camptonites means that a subduction component was not involved in the enrichment process of the source region. However, mantle metasomatism has also been attributed to partial melts and/or metasomatic fluids that migrate from the asthenospheric mantle and freeze in thin zones within the mechanical boundary layer of the continental lithosphere for long periods of geological time (McKenzie, 1989). Re-melting of the metasomatic zone, consisting of veins (with clinopyroxene, amphibole ± mica ± apatite ± carbonate ± oxides) enriched in volatiles and incompatible elements hybridised with variable amounts of partial melts from their less enriched peridotite wall rock, can produce alkaline magmas (e.g. Foley, 1992). Partial melting of the phlogopite-bearing mantle would generate potassic magmas with $K_2O/Na_2O>1$ (Wilson

and Downes, 1991). High Na/K ratios of the Ditrău camptonites suggest that the metasomatic mineral in the source region was rather amphibole than phlogopite. The presence of pargasitic amphibole in the source region can account for the high Nb–Ta concentrations observed in the studied camptonites (Table 1) since the Nb/Ta ratio in the melt is controlled by amphibole during melting, as shown by Tiepolo et al. (2000).

The extremely low Zr/Hf ratio (21.0–32.2) and the positive correlation of Zr/Nb with the Zr concentration (Fig. 7) (also) indicates an enrichment process which could be produced if a constant amount of Nb is added to the variably depleted source region (Weyer et al., 2003). The low Zr/Nb ratio (0.7–5.3) confirms the strong enrichment of incompatible trace elements (Tappe et al., 2006). High initial $^{143}Nd/^{144}Nd$ ratios (ε_{Nd} values of +4.0 to +6.1) of the Ditrău camptonites indicate that the analysed lamprophyre has experienced time-integrated enrichment in Sm or loss of Nd, relative to CHUR (Rock, 1991).

Figure 9 shows the initial ε_{Nd} values vs La/Nb ratios of the camptonites and other igneous rocks from the Ditrău Alkaline Massif, together with fields for HIMU (Zindler and Hart, 1986; Weaver, 1991), alkaline lamprophyres from Moravia (Dostal and Owen, 1998; Harangi et al., 2003), the Spanish Central System (Orejana et al., 2008), the Tamazert Complex (Bernard-Griffiths et al., 1991), the Mecsek-Alföld Igneous Field (Harangi et al., 2003) and the worldwide average (Rock, 1991) for comparison. Ditrău camptonites are within or plot near to the fields of the alkaline lamprophyres from Moravia, the Tamazert alkaline complex and the Spanish Central System (group of PREMA-like dykes). Camptonites from the Spanish Central System are differentiated into an isotopically depleted (PREMA-like) and an isotopically enriched (BSE-like) groups (Orejana et al., 2008). The depleted isotopic signatures have been interpreted with the involvement of a sub-lithospheric source (probably asthenospheric-related) and the enriched isotopic compositions have been explained by participation of a lithospheric mantle. The close similarity to the isotopically depleted Spanish

lamprophyres suggests a sub-lithospheric mantle source for the Ditrău camptonites as well. In the source region of the Moravian, Mecsek-Alföld and Tamazert lamprophyres, the HIMU OIB mantle component has been identified (Bernard-Griffiths et al., 1991; Dostal and Owen, 1998; Harangi et al., 2003). Ditrău camptonites fall near to the field of the HIMU OIB mantle component, as well as the alkaline lamprophyres mentioned above, proposing that a HIMU-type mantle source was involved in the generation of the studied lamprophyres which is consistent with a sub-lithospheric–asthenospheric origin. The relatively homogeneous Nd isotopic compositions with slight differences can also be compatible with variable partial melting of a homogeneous mantle source as suggested by Bernard-Griffiths et al. (1991). REE and Nd isotopic compositional fields for camptonite–I and camptonite–II overlap (Figs. 8 and 9), inferring that they were generated from similar mafic alkaline magma batches of the metasomatised zone in the mantle source with only slight differences in their modal mineralogy (e.g. Orejana et al., 2008).

6.2. Partial melting

To evaluate the generation of such an enriched camptonitic magma, partial melting calculations have been undertaken on garnet (curve A) and spinel (curve B) peridotite mantle sources (according to Kostopoulos and James, 1992) using non-modal batch melting equations integrated with a melting model of an enriched asthenospheric mantle source (EAM) (Seghedi et al., 2004). Melting curves using EAM as the source material have been calculated for different mantle facies including garnet lherzolite (Kostopoulos and James, 1992, curve C), garnet-amphibole lherzolite (Barry et al., 2003, curve D) and another garnet-amphibole lherzolite with slightly different composition than the latter (new calculations, curve E) (Fig. 10). The calculations suggest 1–4% degrees of partial melting of an enriched garnet peridotite mantle source with Ol (58%), Opx (18%), Cpx (13.4%), Grt (6.6%) and

Amph (4.0%). Four percent of amphibole in the modal mineralogy of the source region can explain the volatile enrichment in the primary magma. The composition of samples VRG7292 and VRG7299 (Table 1) may represent this primary magma. Morogan et al. (2000) also point to the hydrous nature of the Ditrau magmas and their generation by small degrees of melting of asthenospheric garnet lherzolite. A small to moderate degree of fractional crystallisation (F_{max}=46.8) for the generation of Ditrău camptonites is also indicated by 4% melting of the enriched garnet-amphibole lherzolite mantle source (Fig. 10). This melt generation corresponds to approximately 80 km depth.

6.3. Fractional crystallisation

Some samples of the Ditrău camptonites (VRG7292, VRG7296 and VRG7297) containing ca. 15% olivine pseudomorphs and ca. 10% clinopyroxene phenocrysts fulfil the compositional criteria for identifying primary upper-mantle partial melts with concentrations of mg#=0.7, Cr=277 ppm, and Ni=214 ppm. However, all the other Ditrău camptonites show various whole-rock mg values (0.44 to 0.70), generally low concentrations of Ni and Cr (6–74 ppm and 4–100 ppm, respectively), indicating that they have undergone variable fractional crystallisation during their ascent, and were probably generated from the more primitive camptonites. The distribution of whole-rock major and trace elements together with the petrographic observations suggest the fractionation of olivine and clinopyroxene in the range of mg# between 0.70 and 0.53 in camptonite–I. During this stage TiO_2 increases and starts to decrease, together with V, from mg# 0.55, while the CaO, FeO^t and Yb/Eu ratios decrease during differentiation which indicates crystallisation of kaersutite in camptonite–I and titanite together with hastingsite in camptonite–II.

Correlations between diopside Cr and mg# and between Si and $Ti+Al^{IV}$ indicate a more primitive melt and/or higher temperature at the beginning of crystallisation (Fig. 4). The Ti/Al

ratio falls between 0.125 and 0.250 indicating a relatively high crystallisation pressure (Fig 4). The high Al^{VI} and the slightly high Na p.f.u. content also confirm that they probably crystallised under higher pressure and temperature (e.g. Adam and Green, 1994; Ubide et al., 2012). Based on the high mg# and Cr content (up to 0.81 wt. % Cr_2O_3), and the aluminian-ferroan diopsidic composition of the pyroxenes, it is supposed that they might have crystallised following olivine at 1200–1250 °C (Thompson, 1974) and 10–15 kbar (Aoki and Kushiro, 1968). According to the thermobarometric calculation developed by Putirka (2008) (RiM69_Ch03_cpx_P-T.xls spreadsheet), diopside in camptonite–I was formed under approximately 1220–1300 °C and 12–20 kbar which is comparable to the literature data estimated above. Clinopyroxene with such chemical features can be considered to be a cognate phase in alkali basaltic volcanics (e.g. Wass, 1979) and probably crystallised under upper-mantle conditions, in accordance with the above assessed PT values (Szabó et al., 1993).

In the further process of crystallisation, two distinct groundmass amphiboles formed under slightly different physical conditions. Different thermobarometric methods were applied (RiM69_Ch04_hbld_plag_thermo-jla.xls spreadsheet). The Al-in-hornblende barometry of Hollister et al. (1987) and Schmidt (1992) show 7–9 kbar for the kaersutite core formation and 5.4–6.9 kbar towards the magnesiohastingsite rim; while for hastingsite formation the calculated pressure is 6–9 kbar. The hornblende-plagioclase thermometer, developed by Blundy and Holland (1990) and Holland and Blundy (1994), shows 755–838 ˚C for the kaersutite and 666–779 ˚C for the hastingsite crystallisation temperatures in the studied camptonites. The estimated PT values for amphiboles are consistent with early crystallisation from the ascending magma, as suggested previously based on mineral chemical data. The frequent intergrowth of amphibole with biotite in the groundmass suggests that these OH-bearing Fe-Mg silicates crystallised at the same time.

6.4. Formation of ocelli

Sub-rounded, leucocratic structures, ocelli distinguished from their host by a lower colour index filled with carbonate and/or felsic silicate minerals are common features of lamprophyres and some alkali basalts (e.g. Azbej et al., 2006; Hauser et al., 2010; Szabó et al., 1993; Rock, 1991). Ocelli in igneous rocks have been interpreted as amygdales, nucleation cores of felsic minerals, or vesicles filled by late-stage minerals (e.g. Cooper, 1979; Foley, 1984) or as products of silicate–carbonate or silicate–silicate liquid immiscibility (e.g. Eby, 1980; Ferguson and Currie, 1971; Philpotts, 1976).

Ditrău camptonites contain both silicate–carbonate ocelli (camptonite–I), and silicate ocelli (camptonite–II). Ocelli found in camptonite–I are similar to ocelli described from worldwide lamprophyres (e.g. Azbej et al., 2006; Foley, 1984; Szabó et al., 1993) consisting of carbonate cores rimmed by albite, biotite with opaque minerals or, rarely, titanite (Fig. 3B, F). They are likely to have been formed by the segregation of a CO_2-rich late-stage melt to produce gas vesicles after much of the groundmass had crystallised (Andronikov and Foley, 2001; Azbej et al., 2006). They lack early formed minerals, such as olivine or clinopyroxene which confirms their generation by late-stage segregation processes (Foley, 1984). Tangential alignment of biotites often occurring around ocelli can be interpreted as a result of expansion of gas bubbles in the partially crystallised magma (Phillips, 1973). Carbonate veins intersecting carbonate ocelli and the pilitic pseudomorphs after olivine phenocrysts represent late-stage fluids transported through the fractures of the solidified camptonites (Azbej et al., 2006).

Silicate ocelli in camptonite–II consist of dominantly plagioclase feldspar with minor amounts of amphibole, biotite, titanite and apatite (Fig. 3D, G, H). Ocelli silicates have very similar chemical compositions compared to their groundmass equivalents. The chemical similarity of

the mineral assemblages found in silicate ocelli to those occurring in the groundmass support their similar evolution and is inconsistent with the theory of silicate–silicate liquid immiscibility, but is consistent with the hypothesis that ocelli are segregations of residual interstitial melt as suggested by Bédard (1994), Cooper (1979) and Foley (1984). The texture of the lamprophyres (Fig. 3D) indicates that after about 40–50 % crystallisation, the magmas (of camptonite–II) consisted of euhedral ferromagnesian minerals and interstitial syenomonzonitic to phonolitic melt (Bédard et al., 1988; Bédard, 1994).

The high amount of ocelli in the Ditrău camptonites refers to the high volatile content of the injected magma. The predominance of carbonate minerals over biotite in the camptonite–I ocelli indicates that CO_2 dominated over H_2O during the late-stage of the crystallisation. In camptonite–II, ocelli plagioclase dominates over amphibole and biotite in contrast to the groundmass, suggesting that the role of H_2O was significantly higher during the formation of the groundmass than of the ocelli, because the high volatile content of the alkaline lamprophyre melt suppresses feldspars to the latest stages of crystallisation (Rock, 1991).

6.5. Tectonic setting

Alkaline mafic magmas are usually produced as a response to lithospheric thinning or due to uprising mantle plumes (Wilson, 1993). We use incompatible and rare earth elements, widely accepted as immobile during post-magmatic alteration processes, to define the geotectonic setting in which the Ditrău camptonites were generated. The distribution of HFS elements (Zr, Y and Ti) in Pearce and Cann's (1973) diagram (Fig. 11) and the primitive mantle-normalised REE patterns indicate a within-plate origin for the studied camptonites (Fig. 8D, E) which agree well with the high initial ε_{Nd} values of the Ditrău camptonites typical of enriched intra-plate compositions. According to Leterrier et al.'s (1992) discrimination diagram, the Ti+Cr vs. Ca distribution of clinopyroxene shows an anorogenic setting for the camptonites (Fig. 4).

All these element distributions suggest the relation of Ditrău camptonites to intra-plate magmatic activity which corresponds well with the formation of the massif during an extensional phase associated with a rifted continental margin, as suggested by Kräutner and Bindea (1998). The authors concluded that the massif formed in three main stages in the mid-Triassic and Jurassic, from mantle-derived melts during extensional tectonism on the south-western European passive margin; the final stage of these extensions involved separation of the Bucovino-Getic microplate from the European continental margin. Morogan et al. (2000) also concluded the OIB-like character of the Ditrău magmas and suggested a mantle plume origin as was assumed previously by Dallmeyer et al. (1997).

6.6. Relation to the Ditrău Alkaline Massif

In the north-western part of the Ditrău Alkaline Massif, small ultramafic to mafic bodies occur, consisting of kaersutite peridotite, olivine hornblendite, hornblendite and gabbro. The mineral composition and chemistry of hornblendites and gabbros strongly resemble the studied camptonites. All three possess apatite, titanite, Fe-Ti oxide, clinopyroxene, amphibole, plagioclase, ± olivine and ± biotite. Amphiboles in hornblendite and gabbro are kaersutite grading to hastingsite, magnesiohastingsite and pargasite (Morogan et al., 2000; Pál-Molnár, 2000), comparable to those observed in camptonites. As well as their whole-rock REE (Fig.8), the compositions of diopside in hornblendites ($Di_{63-81}Hd_{14-27}Aeg_{2-10}$; Pál-Molnár, 2000), gabbros ($Di_{72-73}Hd_{16-19}Aeg_{8-12}$; Morogan et al., 2000) and camptonites ($Di_{76-93}Hd_{1-24}Aeg_{1-8}$) also overlap. The ultramafic and mafic rocks are inferred to represent cumulates (Morogan et al., 2000; Pál-Molnár, 2000) and were derived through fractional crystallisation from a basanitic parental magma (Morogan et al., 2000). Based on the trace element, REE and Nd isotopic data (Fig. 9), in conjunction with the petrographic and mineral chemical evidence, the ultramafic and mafic bodies in the Ditrău Alkaline Massif are interpreted, with the studied

camptonites, as a suite of co-magmatic and co-genetic rocks. The Ditrău lamprophyres represent the only basic melt that penetrated throughout the massif and are in close magmatic and genetic relation with the ultramafic and mafic rocks, and, as such, they are defined as parental melts to the igneous body of the Ditrău Alkaline Massif. Morogan et al. (2000) also suggested that large volumes of basanite magma were involved over a long time interval in the formation of the Ditrău complex.

7. Conclusions

Camptonite dykes intrude a wide range of igneous rock of the Ditrău Alkaline Massif, namely hornblendite, diorite, syenite, nepheline syenite and granite. Two amphibole populations are present in the lamprophyres with steady reduction in Yb/Eu, CaO and FeO^t and similar crystallisation conditions. Camptonite–I contains kaersutite formed under 7–9 kbar and 755–838 °C, while hastingsite formation in camptonite–II shows 6–9 kbar and 666–779 °C. In turn, fractionation of olivine and clinopyroxene are observed only in camptonite–I. The aluminian-ferroan diopside is inferred to form under high pressure and temperature, approximately between 12–20 kbar and 1220–1300 °C. Decreasing TiO_2 and V during differentiation is attributed to abundant titanite crystallisation in camptonite–II, while the significant Ti–phase in camptonite–I is kaersutite. The dykes contain silicate–carbonate and silicate ocelli. Calcite–albite ocelli with subordinate biotite and opaque minerals or, rarely, titanite in camptonite–I are most likely to have generated by late-stage segregation processes producing CO_2-rich gas vesicles after much of the groundmass amphibole had crystallised. In camptonite–II, ocelli and groundmass plagioclases have similar compositions. Thus, they had similar evolutions in the melt, so the plagioclase-dominant ocelli are interpreted as segregations of residual syenomonzonitic interstitial melt.

Ditrău camptonites are inferred to have been generated by 1–4 % partial melting of an enriched garnet lherzolite mantle source containing 4% of pargasitic amphibole. The source enrichment is attributed to a sub-lithospheric metasomatic zone consisting of variable amphibole-rich ± carbonate ± oxides ± apatite ± clinopyroxene-bearing veins, which can account for the volatile enrichment in the camptonitic magmas of the strongly to moderately Si-undersaturated grading to Si-saturated character. An asthenospheric HIMU-OIB-type mantle component was also involved in the generation of the camptonite melt. Chemical composition of the Ditrău camptonites corresponds to an intra-plate magmatism, comparable to an extensional phase of the Alpine evolution, from mid-Triassic to Jurassic involving separation of the Bucovino-Getic microplate from the south-western (Bucovinian) European passive margin by the Civcin-Severin rift system, as assumed previously by Kräutner and Bindea (1998), Pál-Molnár and Árva-Sós (1995), and Pál-Molnár (2000).

Ditrău hornblendites, gabbros and diorites show strong mineral and petrochemical similarities with the alkaline lamprophyres, pointing to a petrogenetic relationship. Furthermore, camptonites represent the only basanitic melt penetrating throughout the complex, thus, they are defined as parental melts to the plutonic suites of the Ditrău Alkaline Massif.

Acknowledgements

We are grateful to Carl-Magnus Mörth (ICP-MS), Birgitta Boström and Klára Hajnal (ICP-AES) at Stockholm University for their help with the analyses. We thank Åke Johansson at the Swedish Museum of Natural History in Stockholm for his technical support in TIMS analyses and for his constructive comments on isotopic results. Hans Harrysson at Uppsala University is acknowledged for technical assistance during the analytical work on the microprobe. Special thanks to Csaba Szabó at the Lithosphere Fluid Research Lab (Eötvös University, Budapest) for fruitful discussions in the first phase of the study. We also thank

Teresa Ubide and an anonymous reviewer for constructive suggestions, which helped to improve the quality of this paper. Funding for this research was provided by the Swedish Institute in Stockholm and grants from Synthesys, the EU-funded Integrated Activities Grant and the Hungarian National Science Foundation (Grant No. T046736).

References

Adam, J., Green, T.H., 1994. The effects of pressure and temperature on the partitioning of Ti, Sr and REE between amphibole, clinopyroxene and basanitic melts. Chemical Geology 117, 219-233.

Anastasiu, N., Constantinescu, E., 1982. Tectostructural position of the foidic rocks in the Romanian Carpathians. Revue Roumaine Geologie Geophysique Geographie serie, Geologie 26, 33-44.

Andronikov, A.V., Foley, S.F., 2001. Trace element and Nd-Sr isotopic composition of ultramafic lamprophyres from the East Antarctic Beaver Lake area. Chemical Geology 175, 291-305.

Aoki, K., Kushiro, I., 1968. Some clinopyroxenes from ultramafic inclusions in Dreiser Weiher, Eifel. Contributions to Mineralogy and Petrology 18, 326-337.

Azambré, B., Rossy, M., Albaréde, F., 1992. Petrology of the alkaline magmatism from the Cretaceous North-Pyrenean Rift Zone (France and Spain). European Journal of Mineralogy 4, 813-834.

Azbej, T., Szabó, C., Bodnar, R.J., Dobosi, G., 2006. Genesis of carbonate aggregates in lamprophyres from the northeastern Transdanubian Central Range, Hungary: Magmatic or hydrothermal origin? Mineralogy and Petrology 88, 479-497.

Balintoni, I., 1981. The importance of the Ditrau Alcaline Massif emplacement moment for dating of the basement overthrusts in the Eastern Carpathians. Revue Roumaine Géologie, Géophysique, Géographie, série Géologie 25, 89-94.

Barry, T.L., Saunders, A.D., Kempton, P.D., Windley, B.F., Pringle, M.S., Dorjnamjaa, D., Saandar., S., 2003. Petrogenesis of Cenozoic basalts from Mongolia: evidence for the role of asthenospheric versus metasomatized lithospheric mantle sources. Journal of Petrology 44, 5-91.

Beard, A.D., Downes, H., Vetrin, V., Kempton, P.D., Maluski, H., 1996. Petrogenesis of Devonian lamprophyre and carbonatite minor intrusions, Kandalaksha Gulf (Kola Peninsula, Russia). Lithos 39, 93-119.

Bédard, J.H., 1988. Comparative amphibole chemistry of the Monteregian and White Mountain alkaline suites, and the origin of amphibole megacrysts in alkali basalts and lamprophyres. Mineralogical Magazine 52, 91-103.

Bédard, J.H., 1994. Mesozoic east North American alkaline magmatism: Part 1. Evolution of Monteregian lamprophyres, Québec, Canada. Geochimica et Cosmochimica Acta 58, 95-112.

Bernard-Griffiths, J., Fourcade, S., Dupuy, C., 1991. Isotopic study (Sr, Nd, O and C) of lamprophyres and associated dykes from Tamazert (Morocco): crustal contamination processes and source characteristics. Earth and Planetary Science Letters 103, 190-199.

Blundy, J.D., Holland, T.J.B., 1990. Calcic amphibole equilibria and a new amphibole-plagioclase geothermometer. Contributions to Mineralogy and Petrology 104/2, 208-224.

Bouabdli, A., Dupuy, C., Dostal, J., 1988. Geochemistry of Mesozoic alkaline lamprophyres and related rocks from the Tamazert massif, High Atlas (Morocco). Lithos 22, 43-58.

Codarcea, A., Codarcea-Dessila, M., Ianovici, V., 1957. Structura geoloică a masivului de roci alcaline de la Ditrău. Buletin St. Revue Roumaine Géologie, Géophysique, II/3-4, 385-446.

Cooper, A.F., 1979. Petrology of ocellar lamprophyres from western Otago, New Zeland. Journal of Petrology 20, 139-163.

Dallmeyer, D.R., Kräutner, H.G., Neubauer, F., 1997. Middle-late Triassic $^{40}Ar/^{39}Ar$ hornblende ages for early intrusions within the Ditrau alkaline massif, Rumania: Implications for Alpine rifting in the Carpathian orogen. Geologica Carpathica 48, 347-352.

Dalpe, C., Baker, D.R., 1994. Partition coefficients for rare-earth elements between calcic amphibole and Ti-rich basanitic glass at 1.5 Gpa, 1100 degrees C. Mineralogical Magazine 58, 207-208.

Dostal, J., Owen, J.V., 1998. Cretaceous alkaline lamprophyres from northeastern Czech Republic: geochemistry and petrogenesis. Geol Rundsch 87, 67-77.

Downes, H., Balaganskaya, E., Beard, A., Liferovich, R., Demaiffe, D., 2005. Petrogenetic processes in the ultramafic, alkaline and carbonatitic magmatism in the Kola Alkaline Province: A review. Lithos 85, 48-75.

Eby, G.N., 1980. Minor and trace element partitioning between immiscible ocelli-matrix pairs from lamprophyre dykes and sills, Monteregian Hills petrographic province, Quebec. Contributions to Mineralogy and Petrology 75, 269-278.

Fall, A., Bodnar, R. J., Szabó, Cs., Pál-Molnár, E., 2007. Fluid evolution in the nepheline syenites of the Ditrău Alkaline Massif, Transylvania, Romania. Lithos 95, 331-345.

Ferguson, J., Currie, K.L., 1971. Evidence of liquid immiscibility in alkaline ultrabasic dikes at Callander Bay Ontario. Journal of Petrology 12, 561-585.

Foley, S.F., 1984. Liquid immiscibility and melt segregation in alkaline lamprophyres from Labrador. Lithos 17, 127-137.

Foley, S., 1992. Vein-plus-wall-rock melting mechanisms in the lithosphere and the origin of potassic alkaline magmas. Lithos 28, 435-453.

Foley, S.F., Jackson, S.E., Fryer, B.J., Greenough, J.D., Jenner, G.A., 1996. Trace element partition coefficients for clinopyroxene and phlogopite in an alkaline lamprophyre from Newfoundland by LAM-ICP-MS. Geochimica et Cosmochimica Acta 60, 629-638.

Giret, A., Bonin, B., Leger, J.M., 1980. Amphibole compositional trends in oversaturated and undersaturated alkaline plutonic ring-complexes. The Canadian Mineralogist 18, 481-495.

Harangi, Sz., Tonarini, S., Vaselli, O., Manetti, P., 2003. Geochemistry and petrogenesis of Early Cretaceous alkaline igneous rocks in Central Europe: implications for a long-lived EAR-type mantle component beneath Europe. Acta Geologica Hungarica 46/1, 77-94.

Hauser, N., Matteini, M., Omarini, R.H., Pimentel, M.M., 2010. Constraints on metasomatized mantle under Central South America: evidence from Jurassic alkaline lamprophyre dykes from the Eastern Cordillera, NM Argentina. Mineralogy and Petrology 100, 153-184.

Hidas, K., Guzmics, T., Szabó, Cs., Kovács, I., Bodnar, R.J, Zajacz, Z., Nédli, Zs., Vaccari, L., Perucchi, A., 2010. Coexisting silicate melt inclusions and H_2O-bearing, CO_2-rich fluid inclusions in mantle peridotite xenoliths from the Carpathian-Pannonian region (central Hungary). Chemical Geology 274, 1-18.

Holland, T., Blundy, J., 1994. Non-ideal interactions in calcic amphiboles and their bearing on amphibole-plagioclase thermometry. Contributions to Mineralogy and Petrology 116, 433-447.

Hollister, L.S., Grissom, G.C., Peters, E.K., Stowell, H.H., Sisson, V.B., 1987. Confirmation of empirical correlation of Al in hornblende with pressure of solidification of calc-alkaline plutons. American Mineralogist 72, 231-239.

Irvine, T.N., Baragar, W.R.A., 1971. A guide to the chemical classification of the common volcanic rocks. Canadian Journal of Earth Sciences 8, 523-548.

Jacobsen, S.B., Wasserburg, G.J., 1984. Sm-Nd isotopic evolution of chondrites and achondrites. II. Earth and Planetary Science Letters 67, 137-150.

Jakab, Gy. 1988: Geologia Masivului alcalin de la Ditrău. Pallas-Akad., M.-Ciuc.

Kerr, A.C., Khan, M., Mahoney, J.J., Nicholson, K.N., Hall, C.M., 2010. Late Cretaceous alkaline sills of the south Tethyan suture zone, Pakistan: initial melts of the Réunion hotspot? Lithos 117, 161-171.

Koglin, N., Kostopoulos, D., Reischmann, T., 2009. The Lesvos mafic-ultramafic complex, Greece: Ophiolite or incipient rift? Lithos 108, 243-261.

Kostopoulos, D.K., James, S.D., 1992. Parametrization of the melting regime of the shallow upper mantle and the effects of variable lithosperic stretching on mantle modal stratification and trace element concentrations in magmas. Journal of Petrology 33, 665-691.

Kretz, R., 1983. Symbols for rock-forming minerals. American Mineralogist 68, 277-279.

Kräutner, H.G., Bindea, G., 1998. Timing of the Ditrău alkaline intrusive complex (Eastern Carpathians, Romania). Slovak Geological Magazine 4, 213-221.

Leterrier, J., Maury, R.C., Thonon, P., Girard, D., Marchal, M., 1982. Clinopyroxene composition as a method of identification of the magmatic affinities of paleo-volcanic series. Earth and Planetary Science Letters 59, 139-154.

Le Maitre, R.W. (Ed.), 2002. Igneous Rocks. A Classification and Glossary of Terms. Cambridge University Press, Cambridge.

Leake, B.E., Woolley, A.R., Arps, C.E.S., Birch, W.D., Gilbert, M.C., Grice, J.D., Hawthorne, F.C., Kato, A., Kisch, H.J., Krivovichev, V.G., Linthout, K., Laird, J., Mandarino, J.A., Maresch, W.V., Nickel, E.H., Rock, N.M.S., Schumacher, J.C., Smith, D.C., Stephenson, N.C.N., Ungaretti, L., Whittaker, E.J.W., Youzhi, G., 1997. Nomenclature of amphiboles : Report on the Subcommittee on Amphiboles of the International Mineralogical Association, Commission on New Minerals and Mineral Names. American Mineralogist 82, 1019-1037.

Machel, H.G. 2000. Application of cathodoluminescence to carbonate diagenesis, in: Pagel, M., Barbin, V., Blance, P., Ohnenstetter, D. (Eds.), Cathodoluminescence in geosciences. Springer, Berlin/Heidelberg, pp. 271-301.

Mauritz, B., 1912. Adatok a gyergyó-ditrói szienittömzs kémiai viszonyainak ismeretéhez. (Data for the knowledge of chemistry of the Ditrău syenite massif). Matematikai Természettudományi Értesítő 30, 607-631.

McCulloch, M.T. Chappell, B.W., 1982. Nd isotopic characteristics of S- and I-type granites. Earth and Planetary Science Letters 58, 51-64.

McKenzie, D., 1989. Some remarks on the movement of small melt fractions in the mantle. Earth and Planetary Science Letters 95, 53-72.

McKenzie, D., O'Nions, R.K., 1991. Partial melt distributions from inversion of rare earth element concentrations. Journal of Petrology 32, 1021-1091.

Mitchell, R.H., 1994. The lamprophyre facies. Mineralogy and Petrology 51, 137-146.

Morimoto, N., 1988. Nomenclature of Pyroxenes. Mineralogy and Petrology 39, 55-76.

Morogan, V., Upton, B.G.J., Fitton J.G., 2000. The petrology of the Ditrău alkaline complex, Eastern Carpathians. Mineralogy and Petrology 69, 227-265.

Orejana, D., Villaseca, C., Billström, K., Paterson, B.A., 2008. Petrogenesis of Permian alkaline lamprophyres and diabases from the Spanish Central System and their

geodynamic context within western Europe. Contributions to Mineralogy and Petrology 156/4, 477-500.

Pál-Molnár, E., 1994. Petrographical characteristics of Ditró (Orotva) diorites, Eastern Charpathians, Transylvania (Romania). Acta Mineralogica-Petrographica, Szeged 34, 95-109.

Pál-Molnár, E., 2000. Hornblendites and diorites of the Ditrău Syenite Massif. Department of Mineralogy, Geochemistry and Petrology, University of Szeged, (Ed.), Szeged.

Pál-Molnár, E., 2010. Geology of Székelyland, in: Szakáll, S., Kristály, F. (eds.), Mineralogy of Székelyland, Eastern Transylvania, Romania, pp. 33-43.

Pál-Molnár, E., Árva-Sós, E., 1995. K/Ar radiometric dating on rocks from the northern part of the Ditrău Syenite Massif and its petrogenetic implications. Acta Mineralogica-Petrographica, Szeged 36, 101-116.

Palme, H., O'Neill, H.S.C., 2004. Cosmochemical estimates of mantle composition, in: Carlson, R.W. (ed.), The Mantle and Core. Treatise on Geochemistry, in: Holland, H.D., Turekian, K.K. (eds.), Volume 2, Elsevier, Oxford, pp. 1-38.

Pană, D., Balintoni, I., Heaman, L., 2000. Precise U-Pb zircon dating of the syenite phase from the Ditrău Alkaline Igneous Complex. Studia Universitatis Babeş-Bolyai, Geologia 45/1, 79-89.

Pearce, J.A., Cann, J.R., 1973. Tectonic setting of basaltic rocks determined using trace element analyses. Earth and Planetary Science Letters 19, 290-300.

Phillips, W.J., 1973. Interpretation of crystalline spheroidal structures in igneous rocks. Lithos 6, 235-244.

Philpotts, A.R., 1976. Silicate liquid immiscibility: Its probable extent and petrogenetic significance. American Journal of Science 276, 1147-1177.

Putirka, K., 2008. Thermometers and Barometers for Volcanic Systems. In: Putirka, K., Tepley, F. (Eds.), Minerals, Inclusions and Volcanic Processes, Reviews in Mineralogy and Geochemistry, Mineralogical Society of America 69,61-120.

Rock, N.M.S., 1991. Lamprophyres. Blackie and Son, Glasgow.

Săndulescu, M., 1984. Geotectonica României. Ed. Tehn., Bucureşti.

Schmidt, M.W., 1992. Amphibole composition in tonalites as a function of pressure: an experimental calibration of the Al-in-hornblende barometer. Contributions to Mineralogy and Petrology 110, 304-310.

Seghedi, I., Downes, H., Vaselli, O., Szakács, A., Balogh, K., Pécskay, Z., 2004. Post-collisional Tertiary-Quaternary mafic alkalic magmatism in the Carpathian-Pannonian region: a review. Tectonophysics 393, 43-62.

Srivastava, R.K., Chalapathi Rao, N.V., 2007. Petrology, geochemistry and tectonic significance of Palaeoproterozoic alkaline lamprophyres from the Jungel Valley, Mahakoshal supracrustal belt, Central India. Mineralogy and Petrology 89, 189-215.

Streckeisen, A., 1954. Das Nephelinsyenit-Massiv von Ditro (Siebenbürgen), II. Teil. Schweizerische Mineralogische Petrographische Mitteilungen 34, 336-409.

Streckeisen, A., 1960. On the structure and origin of the Nepheline-Syenite Complex of Ditro (Transsylvania, Romania). Rep 21th IGC Part 13: 228-238.

Streckeisen, A., Hunziker, J.C., 1974. On the origin of the Nephelinsyenit Massif of Ditró (Transylvania, Romania). Schweizerische Mineralogische Petrographische Mitteilungen 54, 59-77.

Sun, S., McDonough, W.F., 1989. Chemical and isotopic systematics of ocean basalts: implications for mantle composition and process, in: Saunders, A.D., Norry, M.J. (Eds.), Magmatism in the ocean basins, Geological Society Special Publication 42, pp. 313-346.

Szabó, Cs., Kubovics, I., Molnár, Zs., 1993. Alkaline lamprophyre and related dyke rocks in NE Transdanubia, Hungary: The Alcsutdoboz-2 (AD-2) borehole. Mineralogy and Petrology 47, 127-148.

Tappe, S., Foley, S.F., Jenner, G.A., Heaman, L.M., Kjarsgaard, B.A., Romer, R.L., Stracke, A., Joyce, N., Hoefs, J., 2006. Genesis of ultramafic lamprophyres and carbonatites at Aillik Bay, Labrador: a consequence of incipient lithospheric thinning beneath the North Atlantic Craton. Journal of Petrology 47, 1261-1315.

Thompson, R.N., 1974. Some high-pressure pyroxenes. Mineralogical Magazine 39, 768-787.

Tiepolo, M., Vannucci, R., Oberti, R., Foley, S.F., Bottazzi, P., Zanetti, A., 2000. Nb and Ta incorporation and fractionation in titanian pargasite and kaersutite: crystal-chemical constraints and implications for natural systems. Earth and Planetary Science Letters 176, 185-201.

Ubide, T., Arranz, E., Lago, M., Larrea, P., 2012. The influence of crystal settling on the compositional zoning of a thin lamprophyre sill: A multi-method approach. Lithos 132-133, 37-49.

Upton, B.G.J., 1965. The petrology of camptonite sill in south Greenland. Meddelelser om Grønland 169.

Vendl, M., 1926. Telérkőzetek a ditrói nefelinszienit masszívumból (Dykes from the Ditrău syenite massif). Matematikai Természettudományi Értesítő 43, 215-243.

Wass, S.Y., 1979. Multiple origin of clinopyroxenes in alkali basaltic rocks. Lithos 12, 115-132.

Weaver, B.L., 1991. The origin of ocean-island basalt end-member compositions: trace element and isotopic constrains. Earth and Planetary Science Letters 104, 381-397.

Weyer, S., Münker, C., Rehkämper, M., Mezger, K., 2002. Determination of ultra-low Nb, Ta, Zr, and Hf concentrations and the chondritic Zr/Hf and Nb/Ta ratios by isotope dilution analyses with multiple collector ICP-MS. Chemical Geology 187, 295-313.

Weyer, S., Münker, C., Mezger, K., 2003. Nb/Ta, Zr/Hf and REE in the depleted mantle: implication for the differentiation history of the crust-mantle system. Earth and Planetary Science Letters 205, 309-324.

White, W.M., 2009. Geochemistry. http://imwa.info/white-geochemistry.html

Wilson, M., 1993. Magmatism and the geodynamics of basin formation. Sedimentary Geology 86, 5-29.

Wilson, M., Downes, H., 1991. Tertiary-Quaternary extension-related alkaline magmatism in Western and Central Europe. Journal of Petrology 32, 811-849.

Zindler, A., Hart, S.R., 1986. Chemical geodynamics. Annual Review of Earth and Planetary Sciences 14, 493-571.

Figure captions

Fig. 1. (A) Location of the Ditrău Alkaline Massif in the structural system of the Alpine–Carpathian–Dinaric region (Pál-Molnár, 2010). (B) Schematic geological map of the Ditrău Alkaline Massif. (C) Sample locations in the northern part of the Ditrău Alkaline Massif with the same legend as in figure B.

Fig. 2. (A) Field relation of the camptonite dykes with the wall rock (granite), Ditrău Alkaline Massif, Creangă Mare Creek. (B) Camptonite containing ocelli cut by a carbonate vein, Ditrău Alkaline Massif, Jolotca Creek.

Fig. 3. Characteristic petrographic features of camptonite–I and –II from the Ditrău Alkaline Massif. (A) Clinopyroxene phenocryst extensively replaced by tremolite, actinolite and biotite in camptonite–I VRG7292, 1N. (B) Ocellus containing sparry calcite crystals with biotite in the interior rimmed by albite in camptonite–I VRG7294, 1N. (C) Ocellus plagioclase with epidote core in camptonite–I VRG7297, +N. (D) Silicate ocelli filled with zoned plagioclase, hastingsite inter-grown with biotite and apatite in camptonite–II VRG7305, 1N. (E) and (F) Cathodoluminescence images of large ocellus calcites and veins in camptonite–I VRG7294 showing a lighter orange colour at the rims reflecting their variable Mn and/or REE-content. (G) and (H) BSE images of ocellus hastingsite, biotite, andesine, titanite and calcite partly replaced by barite in camptonite–II VRG7305. Mineral abbreviations are after Kretz (1983).

Fig. 4. Compositional variations in clinopyroxene of camptonite–I from the Ditrău Alkaline Massif. Equation of Ti+Cr=0.08Ca-0.04 is after Leterrier et al., (1992). Full circles: cores; open circles: rims.

Fig. 5. Compositional trends in amphibole for the Ditrău camptonites. Circles: camptonite–I; full squares: camptonite–II groundmass; open squares: camptonite-II phenocrysts.

Fig. 6. Correlation diagrams of major elements vs. mg# for the Ditrău camptonites.

Fig. 7. Correlation diagrams of selected trace elements and trace element ratios vs. mg# and Zr for the Ditrău camptonites.

Fig. 8. Plots of trace element and rare-earth element abundances normalised to primitive mantle (Sun and McDonough, 1989) for (A, D) camptonite–I and (B, E) camptonite–II (this

study). One basanite and one alkali basalt dyke (Morogan et al., 2000), and (C, F) hornblendite and diorite (Pál-Molnár, 2000) from the Ditrău Alkaline Massif, the average for alkaline lamprophyres (Rock, 1991) and OIB (Sun and McDonough, 1989) shown for comparison.

Fig. 9. ε_{Nd} vs La/Nb for the Ditrău camptonites and other igneous rocks from the massif. Initial ε_{Nd} is calculated at the age of 200 Ma. Alkaline lamprophyres (AL) from Moravia (Dostal and Owen, 1998; Harangi et al., 2003), Spanish Central System (Orejana et al., 2008), Tamazert Complex (Bernard-Griffiths et al., 1991), Mecsek-Alföld Igneous Field (Harangi et al., 2003) and the worldwide average given by Rock (1991) shown for comparison as well as fields for HIMU, MORB and EM I (Zindler and Hart, 1986; Weaver, 1991).

Fig. 10. La/Yb vs Yb (ppm) diagram for the Ditrău camptonites. Melting curves for garnet lherzolite (A, C), spinel lherzolite (B) and garnet–amphibole lherzolite (D, E) calculated using a non-modal batch melting equation. Partition coefficients for olivine, orthopyroxene, garnet and spinel are from Kostopoulos and James (1992), for clinopyroxene is according to Foley et al., (1996), and for amphibole follow Dalpe and Baker (1994). Source compositions: for PM (primitive mantle) (curves A, B) according to Palme and O'Neill (2004); for EAM (enriched asthenospheric mantle) (curves C, D, E) according to Seghedi et al., 2004. Initial garnet (curves A, C) and spinel (curve B) lherzolite mantle modal compositions are ol60.1+opx18.9+cpx13.7+grt7.3 and ol57+opx25.5+cpx15+sp2.5; melting modes are ol1.2+opx8.1+cpx36.4+grt54.3 and ol1.2+opx8.1+cpx76.4+sp14.3 (Kostopoulos and James, 1992). Garnet–amphibole lherzolite (Barry et al., 2003, curve D) mantle modal composition is ol55+opx22+cpx15+grt5+amph1; melting mode is ol5+opx5+cpx30+grt20+amph40. Melting curve E (source mode: ol58+opx18+cpx13.4+grt6.6+amph4, melting mode:

ol2+opx7+cpx30+grt21+amph40) indicates that the lamprophyric magma could be generated by 1% to 4 % partial melting of an enriched garnet–amphibole lherzolite mantle source followed by fractional crystallisation (FC). The calculated trend for FC of the camptonitic magma is produced by 4% melting of the enriched garnet–amphibole lherzolite mantle source.

Fig. 11. Ti/100 vs. Zr vs Y*3 distribution following Pearce and Cann (1973) for camptonites from the Ditrău Alkaline Massif. A–B: low K-tholeiites, B: ocean floor basalts, B–C: calc-alkaline basalts, D: within-plate basalts.

Figure 1

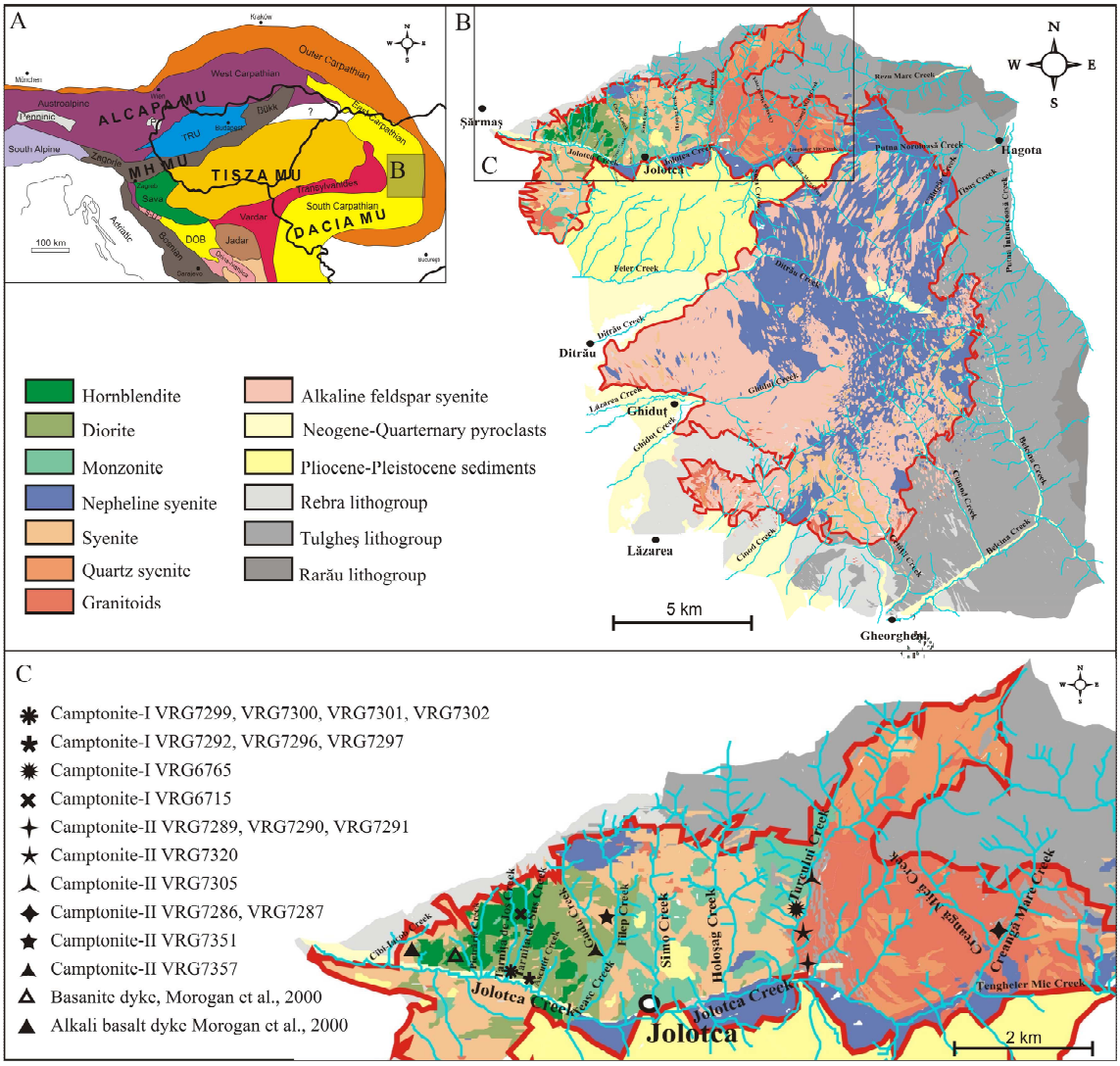

Figure 2

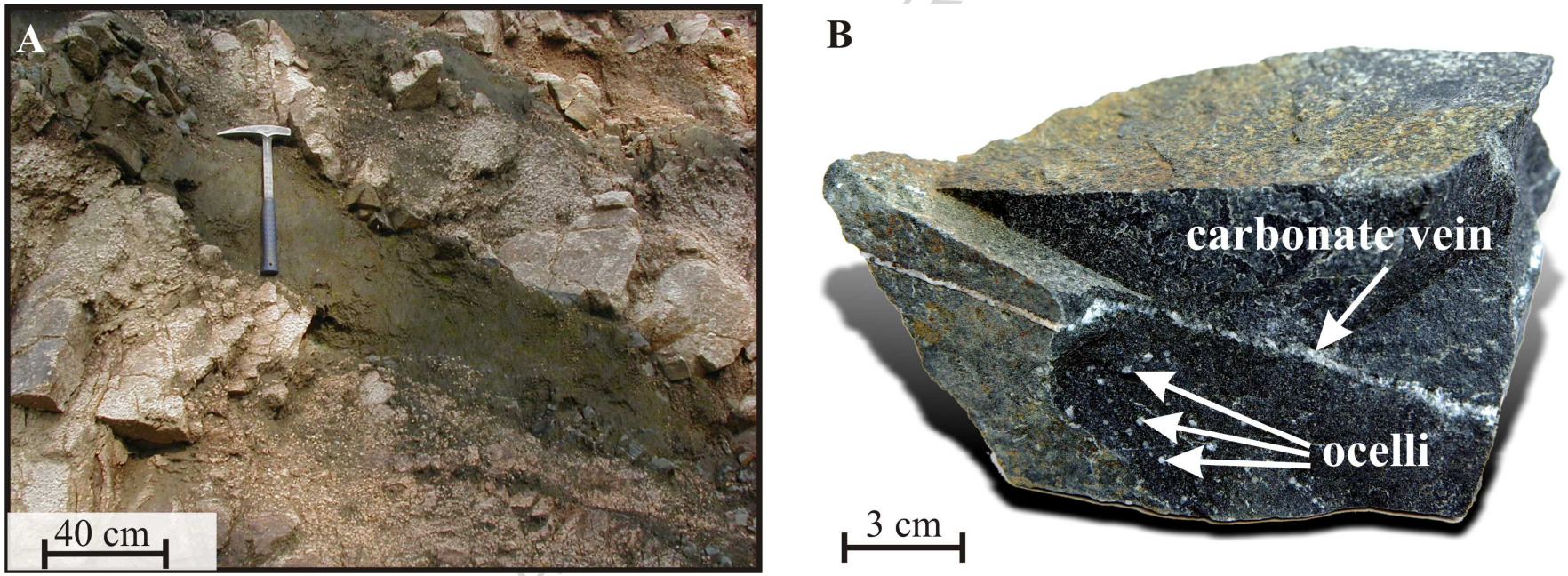

Figure 3

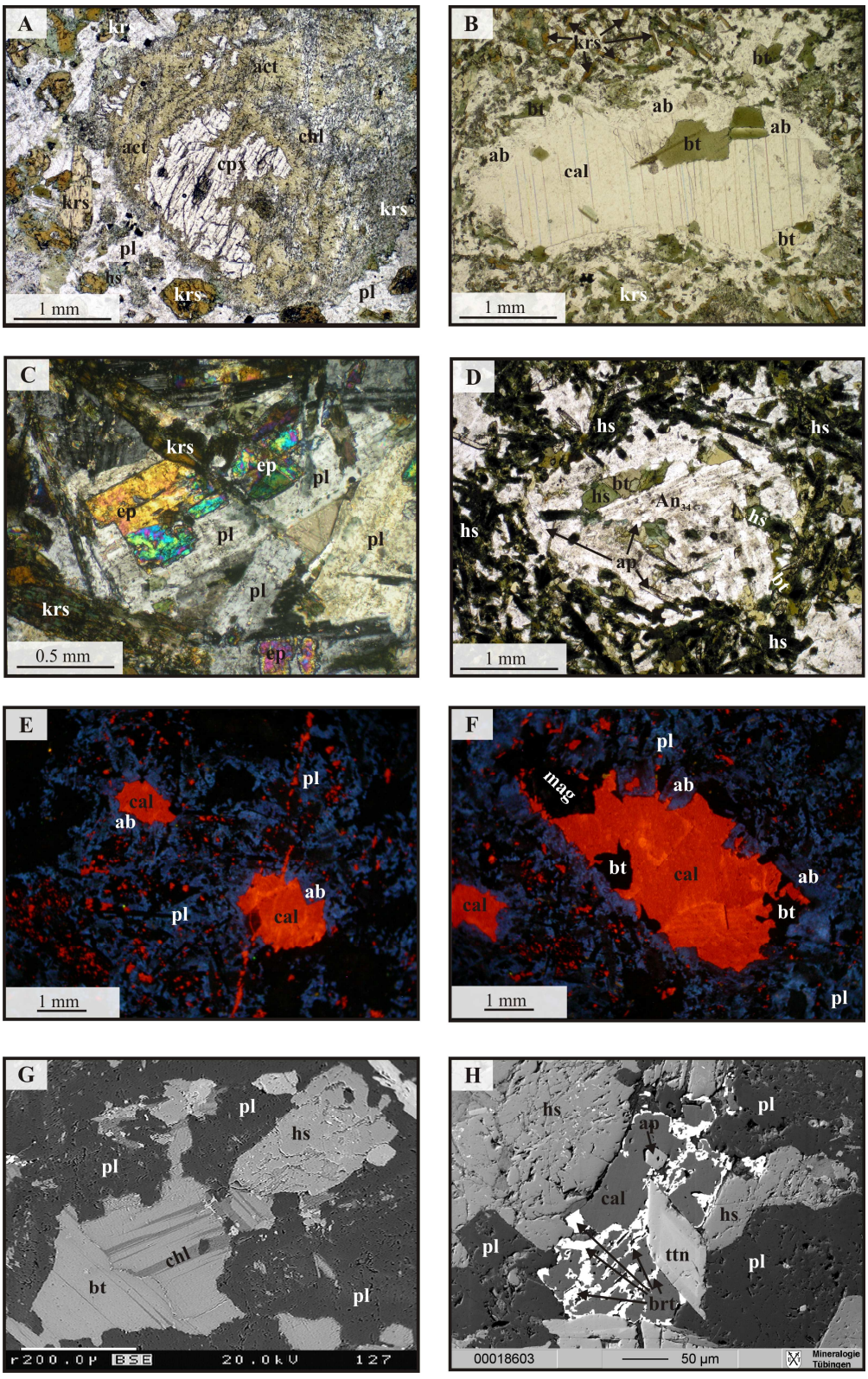

Figure 4

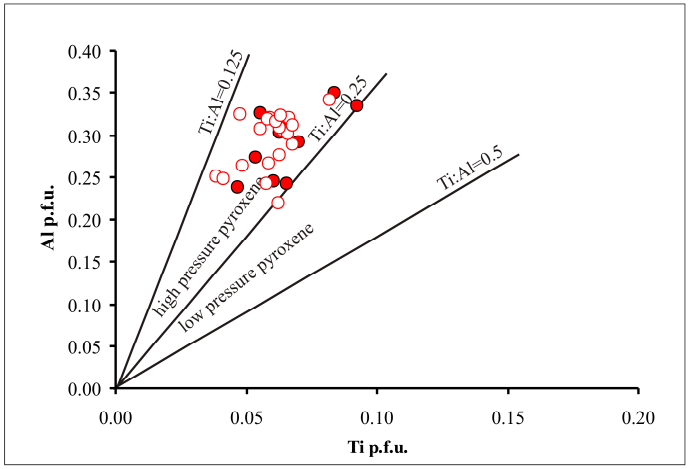

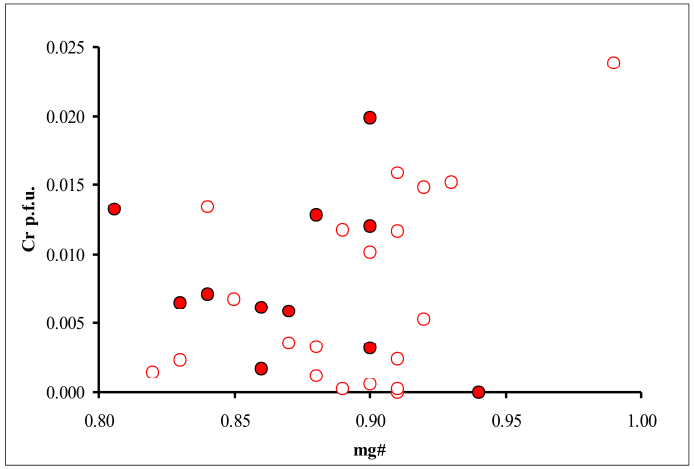

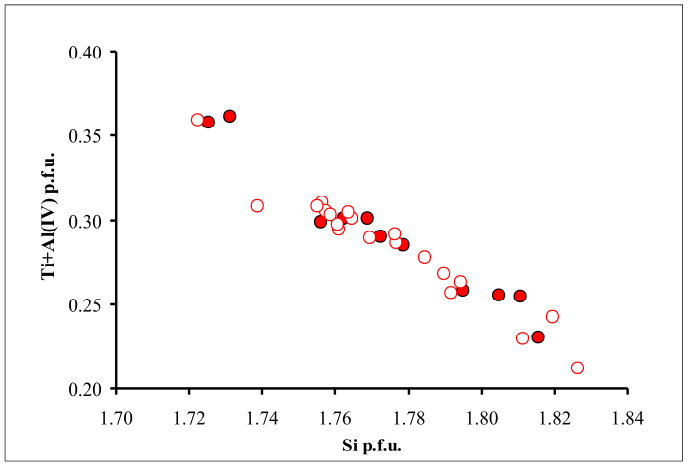

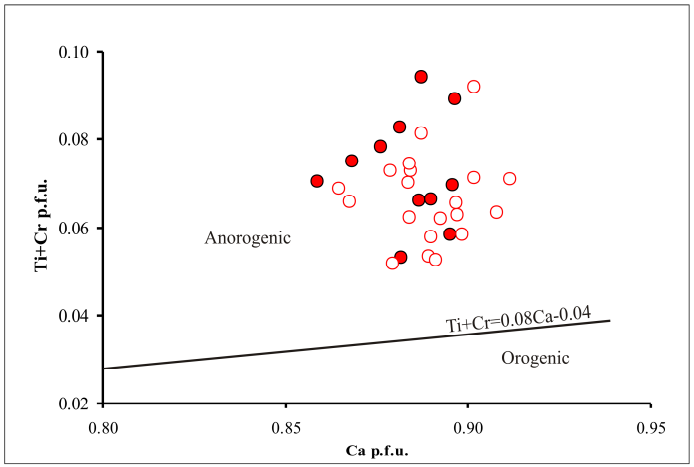

Figure 5

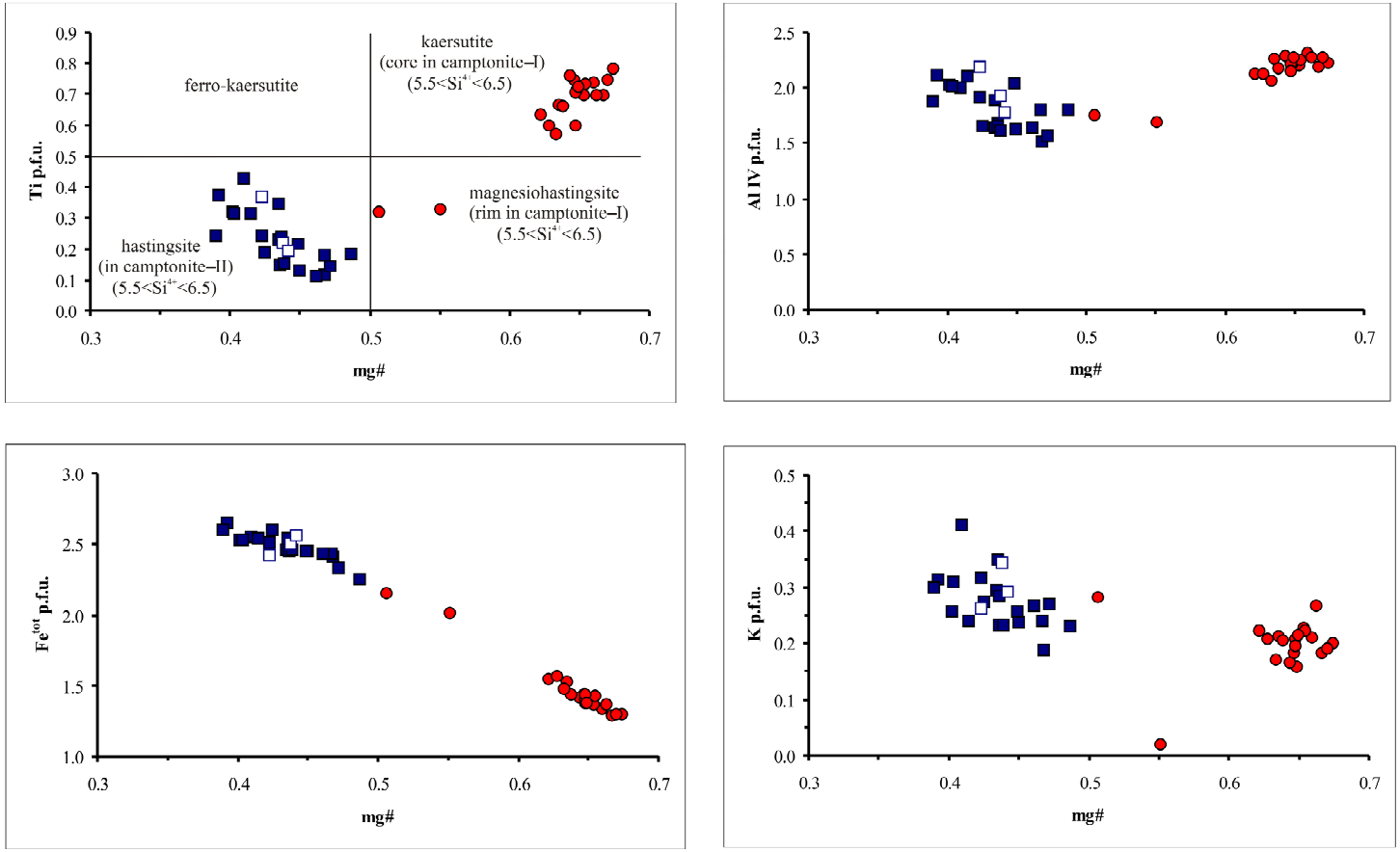

Figure 6

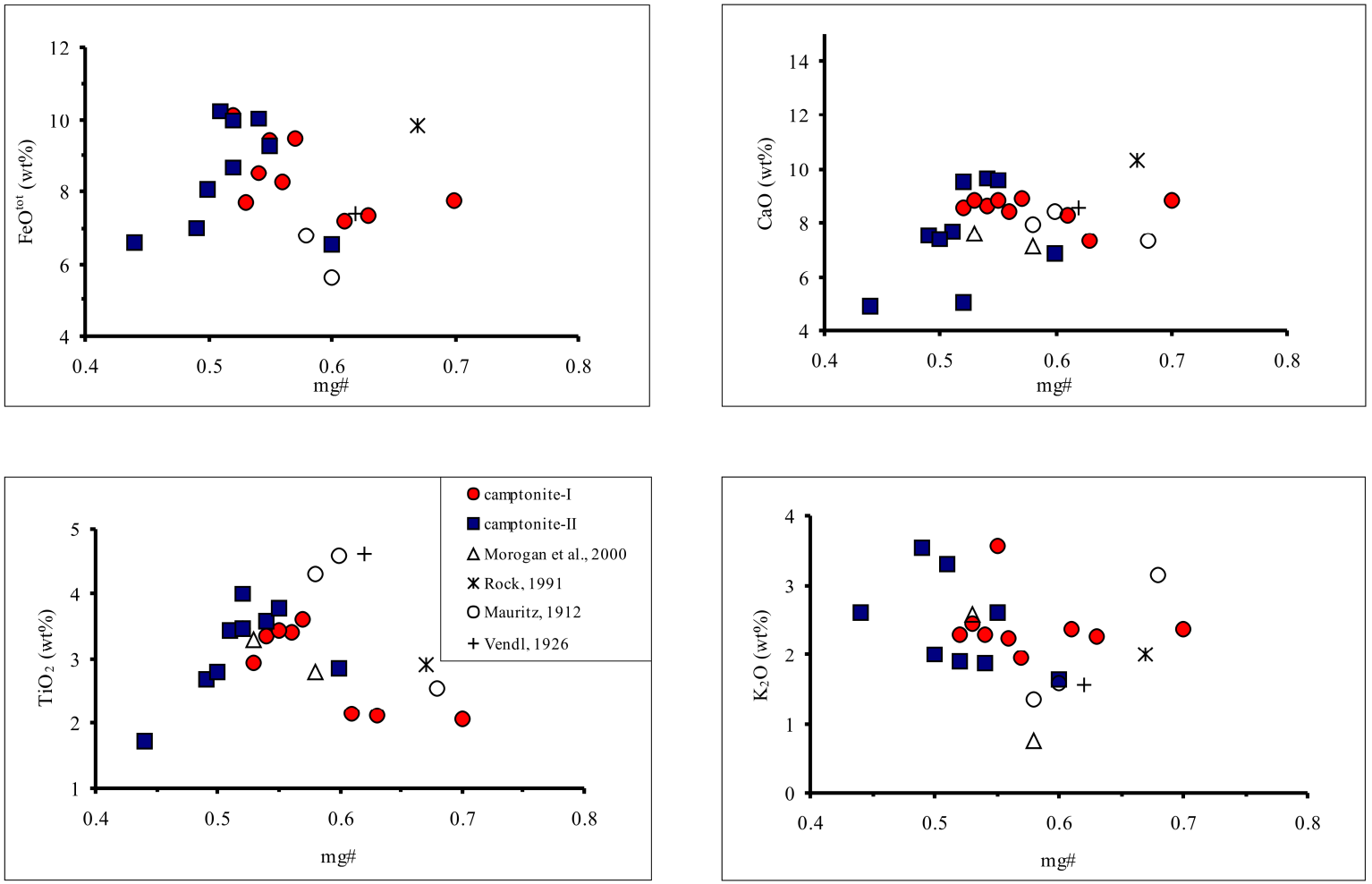

Figure 7

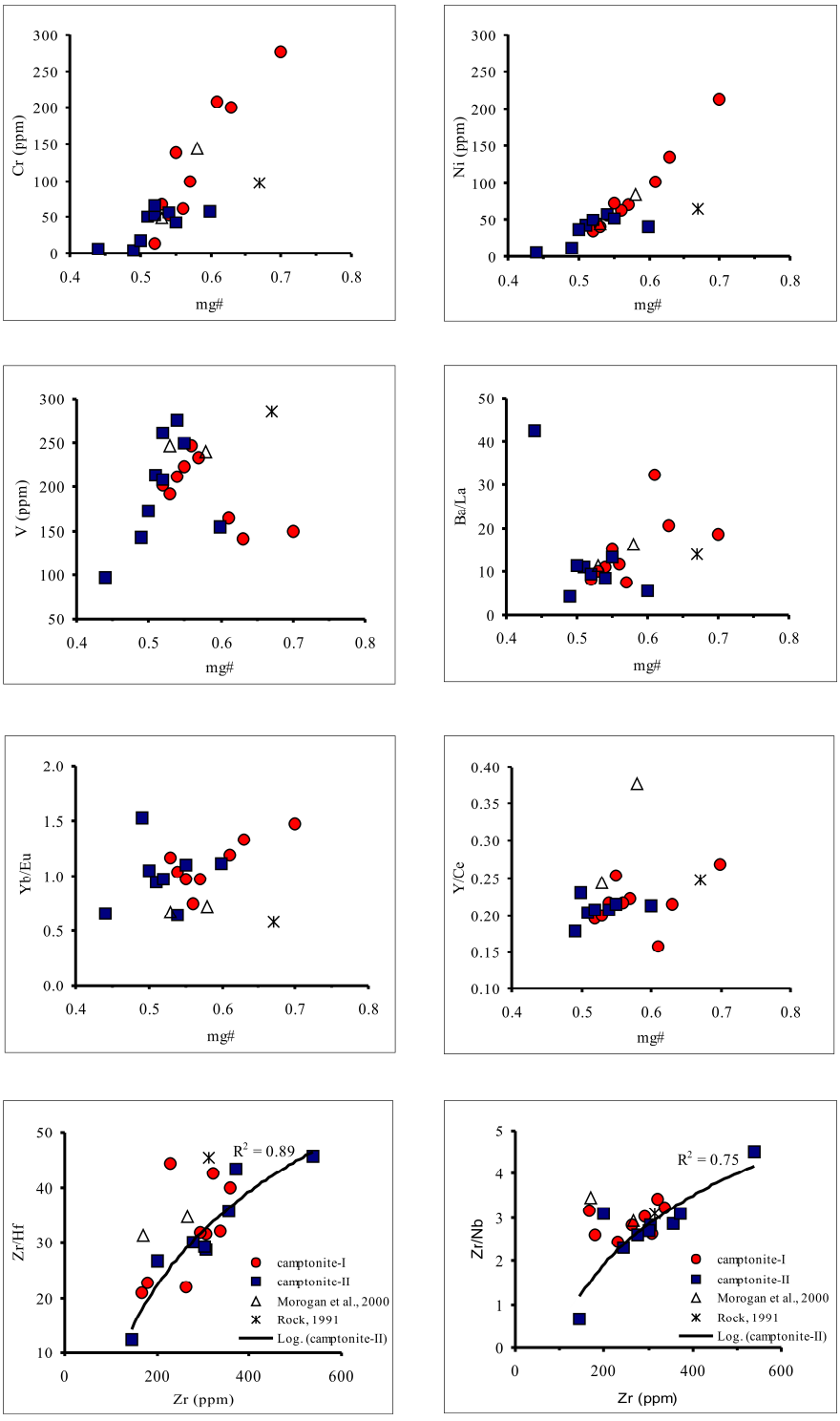

Figure 8

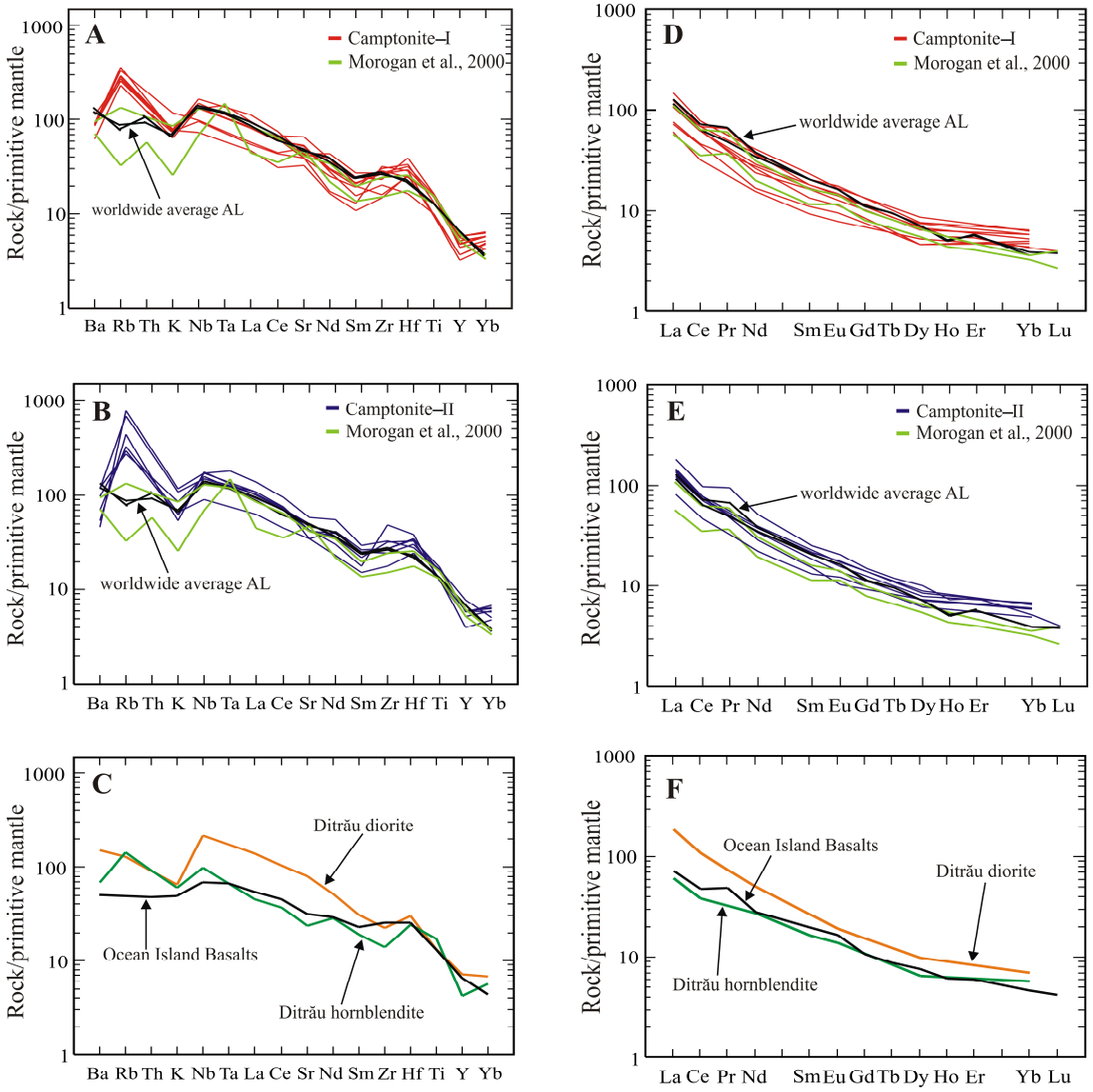

Figure 9

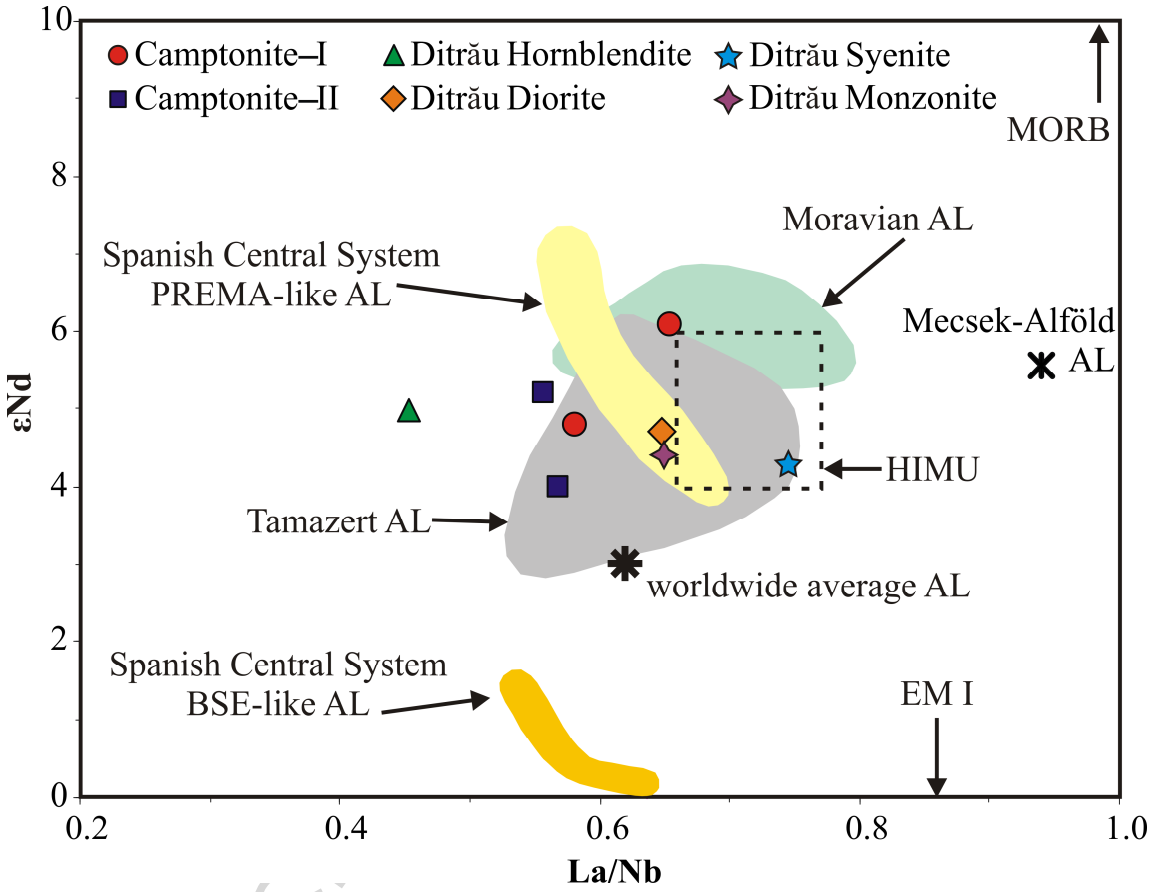

Figure 10

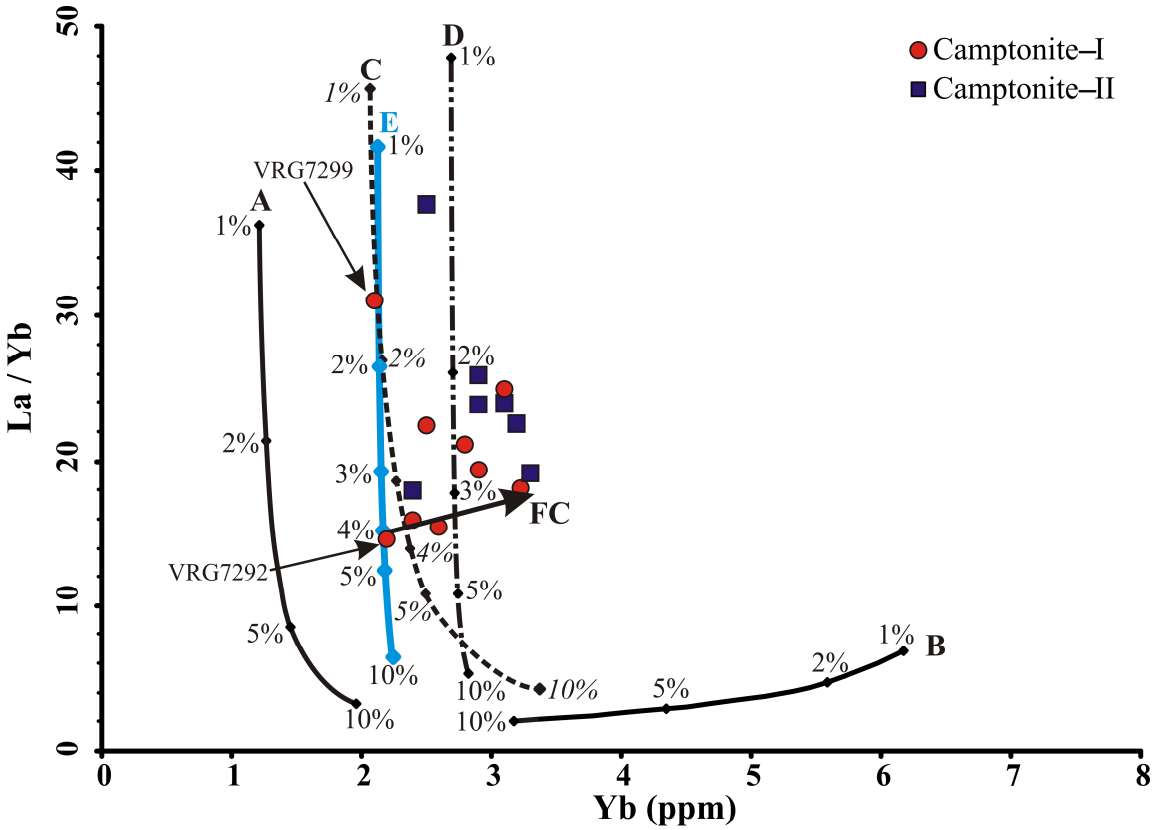

Figure 11

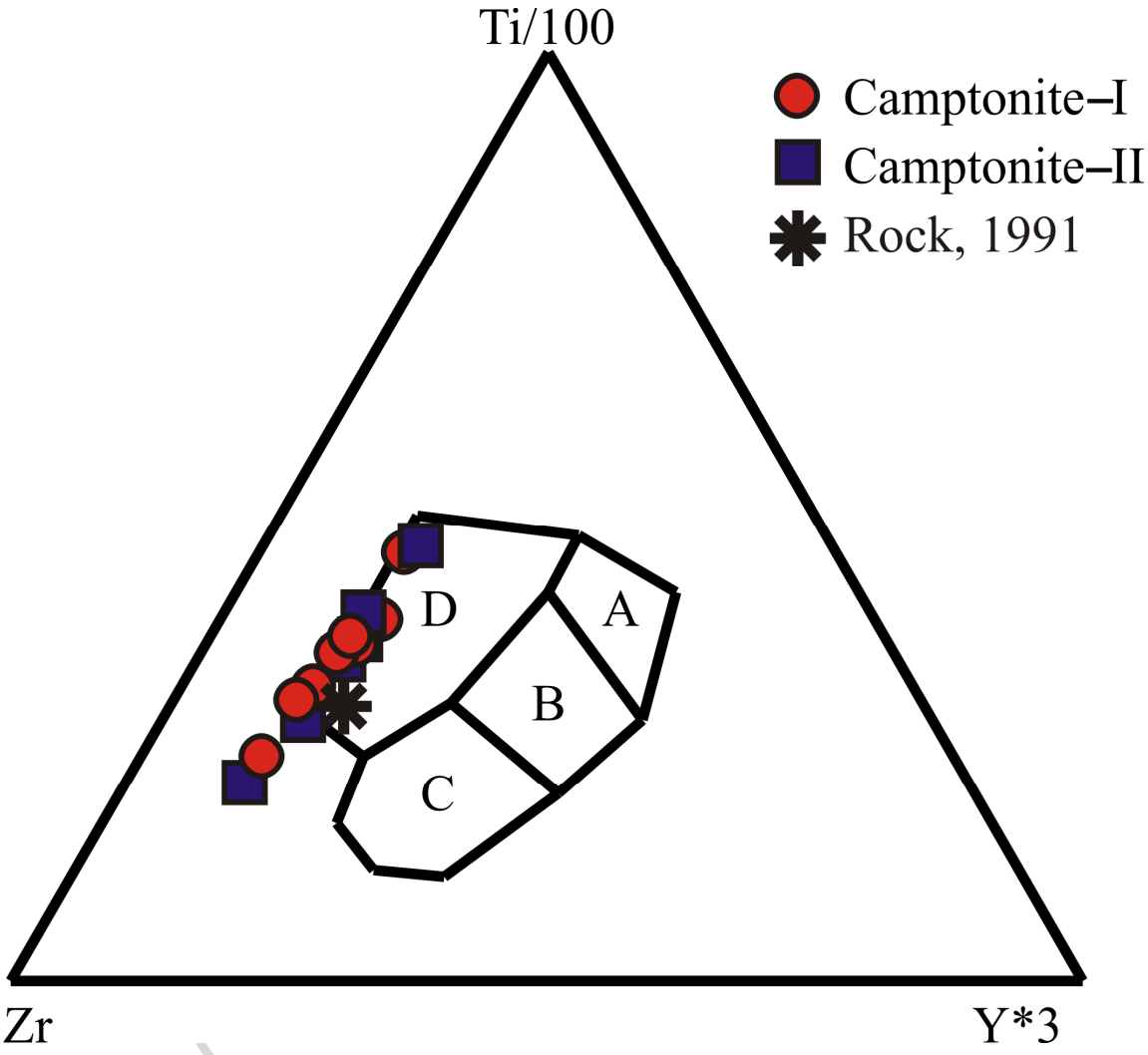

Table 1. Whole-rock analyses of camptonites from the northern part of the Ditrău Alkaline Massif

Location	Tarnica Creek	Török Creek	Jolotca Creek	Jolotca Creek	Jolotca Creek	Tarnica Creek	Tarnica Creek	Tarnica Creek	Tarnica Creek	Nagyág Creek	Nagyág Creek	Török Creek	Török Creek
Sample	VRG	VRG	VRG	VRG	VRG	VRG	VRG	VRG	VRG	VRG	VRG	VRG	VRG
nr.	6715	6765	7292	7296	7297	7299	7300	7301	7302	7286	7287	7289	7290
wt. %	camptonite-I									camptonite-II			
SiO_2	45.29	41.79	45.22	46.26	48.61	45.63	46.46	43.27	46.54	48.39	50.80	44.35	43.32
TiO_2	3.59	3.47	2.07	2.16	2.12	3.40	3.34	3.42	2.93	2.68	2.85	3.42	3.45
Al_2O_3	14.7	14.64	12.52	15.68	15.16	15.39	15.97	14.47	16.07	18.20	16.67	15.42	14.82
Fe_2O_3	2.49	2.60	1.88	1.80	1.81	2.22	2.25	2.45	2.03	1.84	1.78	2.61	2.57
FeO	9.46	10.15	7.73	7.21	7.33	8.26	8.49	9.42	7.71	6.98	6.52	10.24	9.98
MnO	0.16	0.25	0.16	0.17	0.15	0.17	0.17	0.20	0.18	0.27	0.18	0.26	0.25
MgO	7.05	6.24	10.01	6.52	7.14	6.01	5.63	6.60	4.87	3.79	5.37	5.91	6.01
CaO	8.88	8.54	8.85	8.28	7.30	8.43	8.62	8.83	8.79	7.53	6.83	7.68	9.49
Na_2O	3.99	3.57	3.01	4.56	4.49	4.28	4.40	3.02	4.08	4.12	5.35	2.92	3.45
K_2O	1.96	2.29	2.36	2.36	2.25	2.23	2.29	3.57	2.43	3.52	1.63	3.29	1.89
P_2O_5	—	—	—	—	—	0.66	—	—	—	—	—	—	—
LOI	—	—	—	—	—	1.90	—	—	—	—	—	—	—
Total	98.64	95.46	94.67	95.81	97.18	99.50	98.57	96.30	96.49	98.08	98.71	97.25	96.35
mg#	0.57	0.52	0.70	0.61	0.63	0.56	0.54	0.55	0.53	0.49	0.60	0.51	0.52
Normative													
ne	10.8	11.4	8.3	13.8	8.2	10.0	11.8	13.6	9.9	9.5	5.6	8.2	10.3
ol	12.2	14.3	17.6	11.2	13.6	10.9	9.2	11.6	7.6	7.6	9.5	14.2	11.4
ppm													
Be	1.2	2.4	1.2	1.6	1.4	2	1.6	1.1	2.1	4.9	5.2	3.3	2.2
Sc	15.4	14	17.1	12.6	13.3	18	14.9	17.2	13.3	7.1	9.0	12.3	13.4
V	233	202	150	164	142	246	211	224	192	143	155	214	208
Cr	100	13	277	208	201	62	53	138	69	4.1	58	51	53
Co	38	41	45	28	36	38	34	40	30	22	28	32	32
Ni	72	34	214	101	134	63	56	74	41	11.6	40	43	50
Cu	32	41	49	31	51	14	26	32	32	17	22	17	25
Zn	146	141	104	105	104	81	111	146	111	198	145	137	124
Sr	903	931	695	1142	826	1411	1118	1049	837	898	1047	725	875
Ba	442	633	597	1816	781	768	615	620	597	325	377	816	680
Rb	147	229	184	172	174	72	166	215	186	499	279	437	186
Pb						11.6							
Th	—	—	—	—	—	10.6	—	—	—	—	—	—	—
U	—	—	—	—	—	2.8	—	—	—	—	—	—	—
Zr	264	307	168	230	358	322	293	179	338	539	357	306	277
Nb	93	117	53	94	68	94	97	69	105	120	125	108	106
Ta	—	—	—	—	—	5.8	—	—	—	—	—	—	—
Y	26.2	27	14.7	16.9	16.8	26.0	23.6	20.2	21.9	24.1	27.0	27.3	27.0
Hf	12.1	10	8.0	5.2	9.0	7.6	9.2	7.9	10.5	11.8	10.0	10.7	9.2
Mo	4.5	—	7.8	1.9	5.9	1.4	4.0	3.2	7.0	—	11.0	2.8	3.4
S	541	110	595	393	288	—	275	703	566	118	86	87	164
La	58	77	32	56	38	65	56	40	59	75	69	74	72
Ce	118	135	55	107	78	120	109	80	110	135	127	134	130
Pr	—		—	—	—	13.6	—	—	—	—	—	—	—
Nd	53	59	22	38	24	52	41	40	34	40	48	56	54
Sm	11.0	12	4.8	7.0	5.8	9.4	9.4	8.8	8.5	8	9.7	12.0	11.0
Eu	3.3	3.2	1.5	2.1	1.8	2.8	2.8	2.7	2.4	1.9	2.6	3.3	3.3
Gd	—		—	—	—	8.1	—	—	—	—	—	—	—
Tb	—		—	—	—	1.1	—	—	—	—	—	—	—
Dy	5.9	6.6	4.0	3.6	3.6	5.3	5.7	5.1	5.0	5.6	5.4	6.7	6.5
Ho	—		—	—	—	1.0	—	—	—	—	—	—	—
Er	—		—	—	—	2.5	—	—	—	—	—	—	—
Tm	—		—	—	—	0.3	—	—	—	—	—	—	—
Yb	3.2	3.1	2.2	2.5	2.4	2.1	2.9	2.6	2.8	2.9	2.9	3.1	3.2
Lu	—		—	—	—	0.3	—	—	—	—	—	—	—
ΣREE	252	296	122	216	154	284	227	179	222	268	265	289	280

mg#: $Mg/(Mg+Fe^{2+})$, Fe^{2+} calculated according to Irvine and Baragar (1971)

(continued)

Table 1. (continued)

Location	Török Creek	Török Creek	Török Creek	Fülöp Creek	Gudu Creek	Jolotca Creek	Várpatak Creek	Tölgyes road	Várpatak Creek	Jolotca Creek	Jolotca Creek	Average AL
Sample nr.	VRG 7291	VRG 7305	VRG 7320	VRG 7351	VRG 7357	Mauritz, 1912			Vendl, 1926	DT123 Morogan et al., 2000	DT116A Morogan et al., 2000	Rock, 1991
wt. %	camptonite-II									basanite dyke	alk bas dyke	AL average
SiO_2	43.05	46.70	47.84	44.79	50.50	45.97	47.52	48.70	44.66	44.82	47.79	42.5
TiO_2	3.58	4.00	2.78	3.77	1.74	4.59	2.55	4.31	4.62	3.29	2.79	2.90
Al_2O_3	14.81	15.10	16.40	15.64	17.64	17.67	18.00	17.09	14.19	16.01	15.20	13.70
Fe_2O_3	2.60	12.00	2.07	2.49	8.91	4.74	4.26	2.00	3.23	11.09	11.57	12.00
FeO	10.04		8.06	9.28		5.60	3.69	6.80	7.39			
MnO	0.26	0.24	0.15	0.19	0.52	0.11	0.10	0.12	—	0.21	0.17	0.20
MgO	6.50	5.20	4.54	6.41	2.89	4.76	4.46	5.18	6.71	5.04	6.58	7.10
CaO	9.64	5.00	7.38	9.56	4.85	8.43	7.35	7.94	8.52	7.60	7.12	10.30
Na_2O	3.39	3.40	3.92	3.24	5.49	5.87	5.08	4.84	4.04	4.23	4.27	3.00
K_2O	1.87	1.90	2.00	2.59	2.59	1.58	3.14	1.34	1.56	2.56	0.75	2.00
P_2O_5	1.06	0.98	—	—	—	0.09	0.31	0.73	0.64	0.69	0.40	0.74
H_2O	—	—	—	—	—	0.54	2.10	1.29	3.35	—	—	3.10
CO_2	—	—	—	—	—		1.21	—	1.15	—	—	2.00
LOI	1.50	—	—	—	—	—	—	—	—	4.29	3.08	
Total	99.42	94.52	96.05	99.01	95.13	99.95	99.77	100.34	100.06	99.85	99.75	
mg#	0.54	0.52	0.50	0.55	0.44	0.60	0.68	0.58	0.62	0.53	0.58	0.67
Normative												
ne	8.2	0	2.7	10.2	6.2	15.4	12.8	3.5	5.9	10.04	0.24	9.5
ol	13.8	0	10.7	10.7	9.9	2.3	3.5	8.3	8.6	12.5	17.4	13.7
ppm												
Be	4.0	5.4	1.3	1.6	2.1	—	—	—	—	—	—	1.0
Sc	17	—	10.4	16.3	6.6	—	—	—	—	17	21	21.0
V	276	261	173	249	97	—	—	—	—	246	240	285
Cr	56	66	18	42	6	—	—	—	—	48	145	97
Co	37	33	30	37	10	—	—	—	—	—	—	38
Ni	57	—	36	52	6	—	—	—	—	45	85	65
Cu	11	22	39	35	18	—	—	—	—	54	44	50
Zn	74	—	101	126	242	—	—	—	—	124	97	98
Sr	1234	834	723	873	998	—	—	—	—	859	979	990
Ba	799	—	492	851	3020	—	—	—	—	650	494	930
Rb	87	115	206	173	133	—	—	—	—	83	20	50
Pb	3.0					—	—	—	—	2.3	8.0	—
Th	10.1	—	—	—	—	—	—	—	—	8.9	4.8	9.0
Zr	371	244	200	302	144	—	—	—	—	267	169	313
Nb	120	106	65	112	222	—	—	—	—	91	49	101
Ta	7.3	—	—	—	—	—	—	—	—	4.8	5.9	5.0
Y	35.1	29	18.4	26.4	132	—	—	—	—	27	23	31.0
Hf	8.6	—	7.5	10.3	11.6	—	—	—	—	7.7	5.4	6.9
Mo	0.1	—	1.8	2.7	5.5	—	—	—	—	—	—	8.5
S	—	208	82	254	352	—	—	—	—	—	—	—
La	94	—	43	63	71	—	—	—	—	57	30	66
Ce	169	—	80	123	196	—	—	—	—	111	61	125
Pr	19.8	—	—	—	—	—	—	—	—	12.6	7.6	14.0
Nd	74	—	32	50	118	—	—	—	—	45	29	54
Sm	13.1	—	6.8	11.0	37	—	—	—	—	8.6	6.0	10.8
Eu	3.9	—	2.3	3.0	11.9	—	—	—	—	2.7	2.2	3.1
Gd	11.1	—	—	—	—	—	—	—	—	7.5	5.9	8.2
Dy	7.6	—	4.6	6.1	32.6	—	—	—	—	5.0	4.2	5.4
Ho	1.3	—	—	—	—	—	—	—	—	1.0	0.8	0.9
Er	3.4	—	—	—	—	—	—	—	—	2.2	1.9	2.7
Yb	2.5	—	2.4	3.3	7.8	—	—	—	—	1.8	1.6	1.8
Lu	0.3	—	—	—	—	—	—	—	—	0.3	0.2	0.3
ΣREE	400	—	171	259	474	—	—	—	—	255	150	292

Table 2. Rb-Sr and Sm-Nd isotope data for camptonites, hornblendite, diorite, monzonite and syenite of the Ditrău Alkaline Massif, Romania

Rock type	Sample	Rb (ppm)[1]	Sr (ppm)[1]	$^{87}Rb/^{86}Sr$[1]	$^{87}Sr/^{86}Sr \pm 2\sigma_m$[2] (measured)	$^{87}Sr/^{86}Sr$ (initial)	Sm (ppm)[3]	Nd (ppm)[3]	$^{147}Sm/^{144}Nd$[3]	$^{143}Nd/^{144}Nd \pm 2\sigma_m$[4] (measured)	$^{143}Nd/^{144}Nd$ (initial)	ε_{Nd}[5] (initial)
Camptonite–I	VRG6765	229	931	0.7113	0.703512 ± 17	0.70148	13.1	75.6	0.1049	0.512832 ± 30	0.512695	6.1
Camptonite–I	VRG7300	166	1117	0.4294	0.703337 ± 19	0.70211	9.90	53.4	0.1121	0.512773 ± 5	0.512626	4.8
Camptonite–II	VRG7287	278	1047	0.7706	0.703673 ± 27	0.70148	10.8	61.4	0.1063	0.512786 ± 7	0.512647	5.2
Camptonite–II	VRG7351	173	873	0.5731	0.703714 ± 12	0.70208	11.8	64.8	0.1103	0.512729 ± 22	0.512585	4.0
Hornblendite	VRG6745	199	633	0.9092	0.704010 ± 15	0.70142	11.6	60.3	0.1172	0.512791 ± 5	0.512638	5.0
Diorite	VRG6775	65	2146	0.0875	0.702926 ± 13	0.70267	12.3	78.2	0.0950	0.512744 ± 8	0.512620	4.7
Monzonite	VRG6679	284	906	0.9065	0.703755 ± 18	0.70117	4.33	30.3	0.0865	0.512722 ± 11	0.512609	4.4
Syenite	VRG6766	197	566	1.0066	0.704181 ± 26	0.70131	7.08	46.4	0.0923	0.512720 ± 26	0.512599	4.3

1) Rb and Sr contents and $^{87}Rb/^{86}Sr$ ratio from ICP-MS analyses at the Department of Geology and Geochemistry, Stockholm University.

2) $^{87}Sr/^{86}Sr$ ratio corrected for Rb interference and normalised to $^{86}Sr/^{88}Sr = 0.1194$. One run of the NBS SRM 987 Sr standard during the measurement period gave an $^{87}Sr/^{86}Sr$ ratio of 0.710236 ± 24 ($2\sigma_m$). Error given as 2 standard deviations of the mean from the mass spectrometer run int he last digits.

3) Sm and Nd contents and $^{147}Sm/^{144}Nd$ ratio from isotope dilution analysis with combined ^{147}Sm-^{150}Nd tracer. Estimated analytical uncertainty of $^{147}Sm/^{144}Nd$ ratio is ±0.5 %

4) $^{143}Nd/^{144}Nd$ ratios calculated from ID run, corrected to Sm interference and normalised to $^{146}Nd/^{144}Nd = 0.7219$. One run of the La Jolla Nd-standard during the measurement period gave a $^{143}Nd/^{144}Nd$ ratio of 0.511859 ± 11 ($2\sigma_m$). Error given as 2 standard deviations of the mean from the mass spectrometer run in the last digits.

5) Initial ε_{Nd} values (at 200 Ma), according to Jacobsen and Wasserburg (1984): present-day chondritic $^{147}Sm/^{144}Nd$ ratio 0.1967; present-day chondritic $^{143}Nd/^{144}Nd$ ratio 0.512638.

Highlights

1. Ditrău camptonites have been generated by 1–4 % partial melting of an enriched mantle
2. The source region is garnet lherzolite containing 4% of pargasitic amphibole
3. The source enrichment is attributed to a sub-lithospheric metasomatic zone
4. An asthenospheric HIMU-OIB-type mantle component was involved in the melt generation
5. They are deduced to be parental melts to the Ditrău Alkaline Massif